

THE NEURAL CIRCUITRY UNDERLYING THE “RHYTHM EFFECT” IN STUTTERING

1
2
3
4
5
6
7
8
9
10
11
12
13
14
15
16
17
18
19
20
21
22
23
24
25

The neural circuitry underlying the “rhythm effect” in stuttering

Saul A. Frankford¹, Elizabeth S. Heller Murray¹, Matthew Masapollo¹, Shanqing Cai¹, Jason A. Tourville¹, Alfonso Nieto-Castañón¹, and Frank H. Guenther^{1,2,3,4}

¹Department of Speech, Language, & Hearing Sciences, Boston University, Boston, MA 02215

²Department of Biomedical Engineering, Boston University, Boston, MA 02215

³Department of Radiology, Massachusetts General Hospital, Boston, MA 02114

⁴Picower Institute for Learning and Memory, Massachusetts Institute of Technology, Cambridge, MA 02139

Send Correspondence to:

Saul Frankford
Boston University
Department of Speech, Language, & Hearing Sciences
677 Beacon St.
Boston, MA 02215
saulf@bu.edu
(215) 510-7179

THE NEURAL CIRCUITRY UNDERLYING THE “RHYTHM EFFECT” IN STUTTERING

26 **Abstract**

27 **Purpose:** Stuttering is characterized by intermittent speech disfluencies which are dramatically
28 reduced when speakers synchronize their speech with a steady beat. The goal of this study was to
29 characterize the neural underpinnings of this phenomenon using functional magnetic resonance
30 imaging.

31 **Method:** Data were collected from 17 adults who stutter and 17 adults who do not stutter while
32 they read sentences aloud either in a normal, self-paced fashion or paced by the beat of a series
33 of isochronous tones ("rhythmic"). Task activation and task-based functional connectivity
34 analyses were carried out to compare neural responses between speaking conditions and groups.

35 **Results:** Adults who stutter produced fewer disfluent trials in the rhythmic condition than in the
36 normal condition. While adults who do not stutter had greater activation in the rhythmic
37 condition compared to the normal condition in regions associated with speech planning, auditory
38 feedback control, and timing perception, adults who stutter did not have any significant changes.
39 However, adults who stutter demonstrated increased functional connectivity between bilateral
40 inferior cerebellum and bilateral orbitofrontal cortex as well as increased connectivity among
41 cerebellar regions during rhythmic speech as compared to normal speech.

42 **Conclusion:** Modulation of connectivity in the cerebellum and prefrontal cortex during rhythmic
43 speech suggests that this fluency-inducing technique activates a compensatory timing system in
44 the cerebellum and potentially modulates top-down motor control and attentional systems. These
45 findings corroborate previous work associating the cerebellum with fluency in adults who stutter
46 and indicate that the cerebellum may be targeted to enhance future therapeutic interventions.

47
48 **Keywords:** speech production; stuttering; cerebellum; basal ganglia; fMRI; connectivity

THE NEURAL CIRCUITRY UNDERLYING THE “RHYTHM EFFECT” IN STUTTERING

49 **Introduction**

50 Stuttering is a speech disorder that impacts the production of smooth and timely
51 articulations of planned utterances. Stuttering typically emerges early in childhood and persists
52 over the lifespan for 1% of the population (Craig et al., 2009; Yairi & Ambrose, 1999). Speech
53 of people who stutter (PWS) is characterized by perceptually salient repetitions and
54 prolongations of individual phonemes, as well as abnormal silent pauses at the onset of syllables
55 and words accompanied by tension in the articulatory musculature (Max, 2004). These
56 disfluencies are often accompanied by other secondary behaviors such as eye-blinking and facial
57 grimacing (Guitar, 2014). Along with these more overt characteristics, stuttering also has a
58 severe impact on those who experience it, including increased social anxiety and decreased self-
59 confidence, emotional functioning, and overall mental health (Craig et al., 2009; Craig & Tran,
60 2006, 2014). Gaining a better understanding of how and why stuttering occurs will help to lead
61 to more targeted therapies and improve quality of life for PWS.

62 Throughout the years, considerable effort has been made to identify the core pathology
63 underlying stuttering (for reviews, see Max, 2004; Max et al., 2004). More recently, diverse
64 brain imaging modalities have been used to examine how the brains of people who stutter differ
65 from those who do not and how these measures change in different speaking scenarios or
66 following therapy (see Etchell et al., 2018 for a complete literature review). Studies have
67 consistently found that PWS show structural and functional differences in the brain network
68 pertaining to speech initiation and timing (cortico-thalamo-basal ganglia motor loop; Chang &
69 Zhu, 2013; Giraud, 2008; Lu, Peng, et al., 2010) and reduced structural integrity in speech
70 planning areas (left ventral premotor cortex [vPMC] and inferior frontal gyrus [IFG]; Beal et al.,
71 2013, 2015; Chang et al., 2008, 2011; Garnett et al., 2018; Kell et al., 2009; Lu et al., 2012).

THE NEURAL CIRCUITRY UNDERLYING THE “RHYTHM EFFECT” IN STUTTERING

72 Functionally, previous work has indicated that during speech, adults who stutter (AWS) have
73 reduced activation in left hemisphere auditory areas (Belyk et al., 2015; Braun et al., 1997;
74 Chang et al., 2009; De Nil et al., 2000, 2008; Fox et al., 1996; Van Borsel et al., 2003) and
75 overactivation in right hemisphere structures (Braun et al., 1997; De Nil et al., 2000; Fox et al.,
76 1996, 2000; Ingham et al., 2000; Van Borsel et al., 2003), which are typically non-dominant for
77 language processing. These studies strongly suggest that stuttering occurs as the result of
78 impaired speech timing, planning, and auditory processing, and that brain structures not normally
79 involved in speech production are potentially recruited to compensate.

80 In addition to these task activation analyses, previous studies have examined task-based
81 functional connectivity (i.e. activation coupling between multiple brain areas during a speaking
82 task) differences between AWS and ANS. Some studies show reduced connectivity between left
83 IFG and left precentral gyrus in AWS (Chang et al., 2011; Lu et al., 2009), which suggests an
84 impairment in translating speech plans for motor execution (Guenther, 2016). Other studies show
85 group differences in connectivity between auditory, motor, premotor, and subcortical areas (
86 Chang et al., 2011; Kell et al., 2018; Lu, Chen, et al., 2010; Lu et al., 2009; Lu, Peng, et al.,
87 2010). Results of these task-based connectivity studies, as well as resting-state and structural
88 connectivity studies (e.g., Chang & Zhu, 2013; Sitek et al., 2016), have made it apparent that
89 stuttering behavior is not merely the result of disruptions to one or more separate brain regions,
90 but also differences in the ability for brain regions to communicate with one another during
91 speech.

92 In addition to examining neural activation in AWS during typical speech, imaging studies
93 have also looked at activation during conditions where AWS speak more fluently. One such
94 condition that has been widely examined behaviorally is the *rhythm effect* in which stuttering

THE NEURAL CIRCUITRY UNDERLYING THE “RHYTHM EFFECT” IN STUTTERING

95 disfluencies are dramatically reduced when speakers synchronize their speech movements with
96 rhythmic pacing stimuli (Azrin et al., 1968; Barber, 1940; Hutchinson & Norris, 1977; Stager et
97 al., 1997; Toyomura et al., 2011). These fluency-enhancing effects are robust; they occur
98 regardless of whether the pacing stimulus is presented in the acoustic or visual modalities
99 (Barber, 1940), can be induced even by an imagined rhythm (Barber, 1940; Stager et al., 2003),
100 and occur independently of speaking rate (Davidow, 2014; Hanna & Morris, 1977). Previous
101 studies investigating changes in brain activation during the rhythm effect (Braun et al., 1997;
102 Stager et al., 2003; Toyomura et al., 2011, 2015) have found that during rhythmic speech, both
103 AWS and ANS had increased activation in speech-related auditory and motor regions of cortex
104 as well as parts of the basal ganglia. These activation increases were especially pronounced for
105 AWS as compared to ANS. (Toyomura et al., 2011) also demonstrated that these activation
106 increases occurred in regions displaying under-activation during the normal speaking condition.
107 This suggests that pacing speech along with a metronome improves fluency by “normalizing”
108 under-activation in speech production regions. In light of the functional connectivity studies
109 mentioned previously, characterizing changes in brain connectivity between typical and
110 rhythmically-paced speech could illuminate how external pacing leads to normalized activation
111 in the speech network and, ultimately, fluency.

112 In the present study, we employed functional MRI during an overt rhythmic sentence-
113 reading task in AWS and ANS to characterize modulation of brain activation and functional
114 connectivity related to the rhythm effect in stuttering. Meta-analyses in neurotypical adults have
115 implicated a common network for rhythmic perceptual and motor timing (Chauvigné et al., 2014;
116 Wiener et al., 2010) involving the cerebellum, basal ganglia, supplementary motor area, and
117 prefrontal cortex, areas which have been integrated into models of rhythmic processing (Teki et

THE NEURAL CIRCUITRY UNDERLYING THE “RHYTHM EFFECT” IN STUTTERING

118 al., 2012; Zeid & Bullock, 2019). Therefore, we predict that this network, and its connections
119 with auditory and motor areas normally active during speech production, would be recruited to a
120 larger extent during rhythmic compared to normal speech.

121

122 **Method**

123 The current study complied with the principles of research involving human subjects as
124 stipulated by the Boston University institutional review board (protocol 2421E) and the
125 Massachusetts General Hospital human research committee, and participants gave informed
126 consent before taking part. The entire experimental procedure took approximately 2 hours, and
127 subjects received monetary compensation.

128

129 *Subjects*

130 Seventeen AWS (12 males/5 females, aged 18-58 years, mean age = 29.8 years, SD = 12.5 years)
131 and seventeen ANS (11 males/6 females, aged 18-49 years, mean age = 28.7 years, SD = 8.1
132 years) from the greater Boston area were tested. Age was not significantly different between
133 groups (two-sample t-test; $t = 0.31$, $p = 0.759$). Subjects were native speakers of American
134 English who reported normal (or corrected-to-normal) vision and no history of hearing, speech,
135 language, or neurological disorders (aside from persistent developmental stuttering for the
136 AWS). Handedness was measured with the Edinburgh Handedness Inventory (Oldfield, 1971).
137 Using this metric, all AWS were found to be right-handed (scoring greater than 40), but there
138 was more variability among ANS (13 right-handed, 1 left-handed, and 3 ambidextrous). There
139 was a significant difference in handedness score between groups (Wilcoxon rank-sum test; $z =$
140 2.20, $p = 0.028$); therefore, handedness score was included as a covariate in all group imaging

THE NEURAL CIRCUITRY UNDERLYING THE “RHYTHM EFFECT” IN STUTTERING

141 comparisons. For each stuttering participant, stuttering severity was determined using the
142 Stuttering Severity Instrument, Fourth Edition (Riley, 2008); mean score = 23.6, range: 9 to 42;
143 see Table 1 for individual participants). Four additional subjects (3 AWS and 1 ANS) were
144 tested, but they were excluded during data inspection (described below in the *Behavioral*
145 *Analysis* and *Task Activation fMRI Analysis* sections).

146

147 *fMRI Paradigm*

148 Sixteen eight-syllable sentences were selected from the Revised List of Phonetically
149 Balanced Sentences (Harvard Sentences; (*IEEE Recommended Practice for Speech Quality*
150 *Measurements*, 1969; see Appendix). These sentences, composed of one- and two-syllable
151 words, contain a broad distribution of English speech sounds (e.g. “The juice of lemons makes
152 fine punch”). During a functional brain-imaging session, subjects read aloud the stimulus
153 sentences under two different speaking conditions, one in which individual syllables were
154 rhythmically paced by isochronous auditory beats (i.e., the *rhythm* condition), and one in which
155 syllables were produced using a normal (unmodified) speech rate (i.e., the *normal*
156 condition). For each trial, subjects were presented with eight isochronous tones (1000 Hz, 25ms
157 duration) with a 270 ms interstimulus interval. This resulting rate of approximately 222
158 beats/min was chosen so that participants’ speech would approximate the rate of the *normal*
159 condition (based on previous estimates of mean speaking rate in English; (Davidow, 2014;
160 Pellegrino et al., 2004). Participants were instructed to refrain from using any part of their body
161 (e.g., finger or foot) to tap to the rhythm.

162 To avoid confounding interpretation of the BOLD response related to speech production
163 with that of processing the auditory stimulus, the pacing tones were terminated prior to the

THE NEURAL CIRCUITRY UNDERLYING THE “RHYTHM EFFECT” IN STUTTERING

164 presentation of the orthographic stimulus. On *rhythm* trials, subjects used the tones to pace their
165 forthcoming speech, while on *normal* trials, they were instructed to disregard the tones and to
166 read the stimuli at a normal speaking rate, rhythm and intonation. During a *rhythm* or *normal*
167 trial, the orthography of a given sentence was presented with the corresponding trial identifier
168 (i.e., “Rhythm” or “Normal”) presented above the sentence. The font color was either blue for
169 *rhythm* and green for *normal* or vice versa, and colors were counterbalanced across
170 subjects. Subjects were instructed to begin reading aloud immediately after the sentence
171 appeared on the screen. In the event that they made a mistake, they were asked to refrain from
172 producing any corrections and remain silent until the next trial. Silent *baseline* trials were also
173 included wherein subjects heard the tones, and saw a random series of typographical symbols
174 (e.g. ‘+ \ ^ & \$ / [\ \$ = [] * % / - @ \ | - % - / ’) clustered into word-like groupings (matched to stimulus
175 sentences); subjects refrained from speaking during these trials.

176 Subjects participated in a behavioral experiment (not reported here) prior to the imaging
177 experiment that gave them experience with the speech stimuli and the task. The time between
178 this prior exposure and the present experiment ranged from 0 to 424 days. Immediately prior to
179 the imaging session, subjects practiced each sentence under both conditions until they
180 demonstrated competence with the task and sentence production. Subjects also completed a set
181 of six practice trials in the scanner prior to fMRI data collection. To control basic speech
182 parameters across conditions and groups, subjects were provided with performance feedback on
183 their overall speech rate and loudness during practice only. Following this practice set, subjects
184 completed between two and four experimental runs of test trials depending on time constraints
185 (29 completed four, 4 completed three, 1 completed two). During the experimental session,
186 verbal feedback was provided between runs if subjects consistently performed outside of the

THE NEURAL CIRCUITRY UNDERLYING THE “RHYTHM EFFECT” IN STUTTERING

187 specified speech rate (220 ms to 320 ms mean syllable duration). Each run consisted of 16
188 *rhythm* trials, 16 *normal* trials, and 16 *baseline* trials, pseudo-randomly interleaved within each
189 run for each subject. All trials were audio-recorded for later processing.

190

191 *Data Acquisition*

192 MRI data for this study were collected at two locations: the Athinoula A. Martinos Center
193 for Biomedical Imaging at the Massachusetts General Hospital (MGH), Charlestown Campus (9
194 AWS, 9 ANS) and the Cognitive Neuroimaging Center at Boston University (BU; 8 AWS, 8
195 ANS). At MGH, images were acquired with a 3T Siemens Skyra scanner and a 32-channel head
196 coil, while a 3T Siemens Prisma Scanner with a 64-channel head coil was used at BU. At each
197 location, subjects lay supine in the scanner and functional volumes were collected using a
198 gradient echo, echo planar imaging BOLD sequence (repetition time [TR] = 11.5 s, acquisition
199 time = 2.47 s, TE = 30 ms, Flip Angle = 90°). Each functional volume covered the entire brain
200 and was composed of 46 axial slices (64 x 64 matrix) acquired in interleaved order and
201 accelerated using a simultaneous multislice factor of 3 with a 192 mm field of view. The in-plane
202 resolution was 3.0 x 3.0 mm², and slice thickness was 3.0 mm with no gap. Two “dummy” scans
203 were included at the beginning of each run to ensure equilibrium in the magnetic field prior to
204 data collection. Additionally, a high-resolution T1-weighted whole-brain structural image was
205 collected from each participant to anatomically localize the functional data (MPRAGE sequence,
206 256 x 256 x 176 mm³ volume with a 1 mm isotropic resolution, TR = 2.53 s, inversion time =
207 1100 ms, echo time = 1.69 ms, flip angle = 7°).

208 Functional data were acquired using a sparse image acquisition paradigm (Eden et al.,
209 1999; Hall et al., 1999) that allowed participants to produce the target sentences during silent

THE NEURAL CIRCUITRY UNDERLYING THE “RHYTHM EFFECT” IN STUTTERING

210 intervals between volume acquisitions. Volumes were acquired 5.7-8.17 s after stimulus
211 presentation to ensure a 4-6 second delay between the middle of sentence production and the
212 acquisition, in alignment with the delay in the peak of the task-related blood oxygen-level-
213 dependent (BOLD) response (Belin et al., 1999). By scanning after speech production has ended,
214 this paradigm reduces head motion-induced scan artifacts, eliminates the influence of scanner
215 noise on speaker performance, and allows subjects to perceive their own self-generated auditory
216 feedback in the absence of scanner noise (e.g., Gracco et al., 2005). A schematic representation
217 of the trial structure and timeline is shown in Figure 1.

218 Visual stimuli were projected onto a screen viewed from within the scanner via a mirror
219 attached to the head coil. Auditory stimuli were delivered to both ears through Sensimetrics
220 model S-14 MRI-compatible earphones using Matlab (The MathWorks, Natick, MA). Subjects’
221 utterances were transduced with a Fibersound model FOM1-MR-30m fiber-optic microphone,
222 sent to a laptop (Lenovo ThinkPad W540), and recorded using Matlab. Subjects took a short
223 break after completing each run.

224

225 *Behavioral Analysis*

226 An automatic speech recognition engine was used to objectively measure how accurately
227 subjects aligned their syllables to the metronome beats. Specifically, the open-source large-
228 vocabulary continuous speech recognition engine *Julius* (Lee & Kawahara, 2009) was used in
229 conjunction with the free *VoxForge* American English acoustic models (voxforge.org) to
230 perform phoneme-level alignment on the sentence recordings. This resulted in phoneme
231 boundary timing information for every trial. A researcher manually inspected each trial to ensure
232 correct automatic detection of phoneme boundaries. Any trials in which the subject made a

THE NEURAL CIRCUITRY UNDERLYING THE “RHYTHM EFFECT” IN STUTTERING

233 reading error, a condition error (i.e. spoke rhythmically when they were cued to speak normally
234 or vice versa), or a disfluency categorized as a stutter by a licensed speech-language pathologist
235 were eliminated from further behavioral analysis. One ANS that made consistent condition errors
236 was eliminated from further analysis. One AWS was eliminated from further analysis due to an
237 insufficient number of fluent trials during the *normal speech* condition (6/64
238 attempted). Additionally, following the error trial elimination step, behavioral data from AWS13
239 were deleted due to a technical error, so only 16 AWS are included in the behavioral analyses.

240 To evaluate whether there was a fluency-enhancing effect of rhythmic pacing, the
241 percentage of trials eliminated due to stuttering in the AWS group was compared between the
242 two speaking conditions using a non-parametric Wilcoxon signed-rank test. Measures of the total
243 sentence duration and intervocalic timing from each trial were also extracted to determine the
244 rate and isochronicity of each production. Within a sentence, the average time between the
245 centers of the eight successive vowels was calculated to determine the intervocalic interval (IVI).
246 The reciprocal ($1/IVI$) was then calculated, resulting in a measure of speaking rate in units of
247 IVIs per second. The coefficient of variation for intervocalic intervals (CV-IVIs) was also
248 calculated by dividing the standard deviation of IVIs divided by the mean IVI. A higher CV-IVI
249 indicates higher variability of IVI, while a CV-IVI of 0 reflects perfect isochronicity. Rate and
250 CV-IVI were compared between groups and conditions using a mixed design ANOVA. A
251 Bonferroni correction was applied across these two analyses to account for testing these related
252 measures.

253

254 *Task Activation fMRI Analysis*

THE NEURAL CIRCUITRY UNDERLYING THE “RHYTHM EFFECT” IN STUTTERING

255 *Preprocessing:* Following data collection, all images were processed through two
256 preprocessing pipelines: a surface-based pipeline for cortical activation analyses and a volume-
257 based pipeline for subcortical and cerebellar analyses. For the surface-based pipeline, functional
258 images from each subject were simultaneously realigned to the mean subject image and
259 unwarped (motion-by-inhomogeneity interactions) using SPM12’s realign and unwarp procedure
260 (Andersson et al., 2001). Outlier scans were detected with Artifact Detection Tools (ART;
261 https://www.nitrc.org/projects/artifact_detect/) based on motion displacement (scan-to-scan
262 motion threshold of 0.9 mm) and mean signal change (scan-to-scan signal change threshold of 5
263 standard deviations above the mean). Functional images from each subject were then
264 coregistered with their high-resolution T1 structural images and resliced using SPM12’s inter-
265 modal registration procedure with a normalized mutual information objective function. The
266 structural images were segmented into white matter, grey matter, and cerebrospinal fluid, and
267 cortical surfaces were reconstructed using the FreeSurfer image analysis suite (freesurfer.net;
268 Fischl et al., 1999). Functional data were then resampled at the location of the FreeSurfer
269 fsaverage tessellation of each subject-specific cortical surface.

270 For the volume-based pipeline, functional volumes were realigned and unwarped,
271 centered, and run through ART as described for the surface-based pipeline. Functional volumes
272 were then simultaneously segmented and normalized directly to Montreal Neurological Institute
273 (MNI) space using SPM12’s combined normalization and segmentation procedure (Ashburner &
274 Friston, 2005). A mask was then applied such that only voxels within the brain were submitted to
275 subsequent analyses. The original T1 structural image from each subject was also centered,
276 segmented and normalized using SPM12.

THE NEURAL CIRCUITRY UNDERLYING THE “RHYTHM EFFECT” IN STUTTERING

277 Following preprocessing, two AWS were eliminated from subsequent analyses; one due
278 to excessive head motion in the scanner (>1.5mm average scan-to-scan motion) and one due to
279 structural brain abnormalities.

280

281 *First-level Analysis:* After preprocessing, BOLD responses were estimated for each
282 subject using a general linear model (GLM) in SPM12. Because images were collected in a
283 sparse sequence with a relatively long TR, the BOLD response for each trial (event) was
284 modeled as an individual epoch. The model included regressors for each of the conditions of
285 interest: *normal speech*, *rhythm speech*, and *baseline*. Trials that contained reading errors,
286 condition errors, or disfluencies were modeled as a single separate condition of non-interest.
287 Condition regressors were collapsed across runs to maximize power while controlling for
288 potential differences in the number of trials produced without errors or disfluencies. For each
289 run, regressors were added to remove linear effects of time (e.g. signal drift, adaptation) in
290 addition to six motion covariates (taken from the realignment step) and a constant term.
291 Additional regressors were added to remove the effects of acquisitions with excessive scan-to-
292 scan motion or global signal change (taken from the artifact detection step, described above).
293 The first-level model regressor coefficients for the three conditions of interest were estimated at
294 each surface vertex and subcortical voxel, then averaged within anatomical regions of interest
295 (ROIs; see below). The mean *normal speech* and *rhythm speech* coefficients were then
296 contrasted with the *baseline* condition within each ROI to yield contrast effect-size values for the
297 two contrasts of interest (*Normal – Baseline* and *Rhythm – Baseline*) in all ROIs.

298 *Region-of-Interest Definition:* Cortical ROIs were labeled according to a modified
299 version of the SpeechLabel atlas previously described in (Cai et al., 2014); the atlas divides the

THE NEURAL CIRCUITRY UNDERLYING THE “RHYTHM EFFECT” IN STUTTERING

300 cortex into macro-anatomically defined ROIs specifically tailored for studies of speech. Labels
301 are applied by mapping the atlas from the FreeSurfer *fsaverage* cortical surface template to each
302 individual surface reconstruction.

303 Subcortical and cerebellar ROIs were extracted from multiple atlases. Thalamic ROIs
304 were extracted from the mean atlas of thalamic nuclei described by (Krauth et al., 2010). Basal
305 ganglia ROIs were derived from the non-linear normalized probabilistic atlas of basal ganglia
306 (ATAG) described by (Keuken et al., 2014). Each ROI was thresholded at a minimum
307 probability threshold of 33% and combined in a single labeled volume in the atlas’s native space
308 (the MNI104 template). Cerebellar ROIs were derived from the SUI 25% maximum probability
309 atlas of cerebellar regions (Diedrichsen, 2006; Diedrichsen et al., 2009, 2011). Each atlas was
310 non-linearly registered to the SPM12 MNI152 template and then combined into a single labeled
311 volume.

312
313 *Second-Level Group Analyses:* Two sets of analyses were carried out to detect activation
314 differences across groups and conditions: hypothesis-based primary analyses, and exploratory
315 secondary analyses. The primary second-level analyses were carried out on a small set of
316 hypothesis-based *a priori* ROIs (see Figure 2). These included regions belonging to the cortico-
317 basal ganglia-thalamo-cortical motor loop (Guenther, 2016), meta-analyses of rhythmic
318 perceptual and motor timing (Chauvigné et al., 2014; Wiener et al., 2010), and prior
319 neuroimaging studies examining the rhythm effect in stuttering (Stager et al., 2003; Toyomura et
320 al., 2011). Statistical corrections were applied for the number of ROIs tested. The following
321 cortical ROIs in the SpeechLabel atlas were grouped to test our hypotheses: ventral and mid
322 primary motor cortex (MC), ventral and mid premotor cortex (PMC), supplementary motor area

THE NEURAL CIRCUITRY UNDERLYING THE “RHYTHM EFFECT” IN STUTTERING

323 and pre-supplementary motor area (SMA), posterior superior temporal gyrus and planum
324 temporale (pSTg), and ventral and dorsal inferior frontal gyrus pars opercularis (IFo). By
325 grouping the ROIs, we better match the extent of areas shown to be involved in rhythm
326 processing/stuttering in prior reports and increase the sensitivity of our analyses by reducing the
327 number of ROIs.

328 Additional exploratory analyses were performed to determine if activation from other
329 brain regions active during speech production was also modulated by group or condition. For
330 each exploratory analysis, results are reported if they have a p -value less than 0.05, uncorrected.
331 To determine this set of regions, second-level random effects analyses were performed on first-
332 level contrast effect sizes in all ROIs for each group separately. Regions with significant positive
333 activation (thresholded at one-sided $p < 0.05$, and corrected for multiple comparisons using a
334 false discovery rate correction [FDR; Benjamini & Hochberg, 1995] within each contrast) in any
335 of these four contrasts were included in subsequent analyses (see Supplementary Figure 2 and
336 Supplementary Figure 3 for the complete list).

337 Group activation differences were examined in the two speech conditions compared to
338 baseline (*Normal – Baseline*, *Rhythm – Baseline*) as well as the *Group × Condition Interaction*.
339 Additionally, differences between the two speech conditions (*Rhythm – Normal*) were examined
340 in each group separately. These group and condition effects were determined using a
341 GLM. Average subject motion was added as a regressor of non-interest for all analyses. In
342 addition, to account for differences across the two data collection sites, an additional regressor of
343 non-interest was included for all analysis. Due to significant difference in handedness between
344 the two groups (see Subjects section above), handedness score was also included as a regressor
345 of non-interest for between-group and interaction analyses. Finally, to control for stuttering

THE NEURAL CIRCUITRY UNDERLYING THE “RHYTHM EFFECT” IN STUTTERING

346 severity, a modification of the SSI-4 score, heretofore termed “SSI-Mod,” was included as
347 another regressor of non-interest in the between-group and interaction analyses. SSI-Mod
348 removes the secondary concomitants subscore from each subject’s SSI-4 score, thus focusing the
349 measure on speech-related function. The SSI-Mod and SSI-4 composite scores for each subject
350 are included in Table 1. Additional regression analyses were carried out to determine whether
351 stuttering severity, measured by the SSI-Mod, or disfluencies occurring during the experiment
352 were correlated with task activation. Because very few disfluencies occurred during the rhythm
353 condition, we were only able to calculate the correlation between the percentage of disfluencies
354 occurring during *normal* trials (“Disfluency Rate”) and the *Normal - Baseline* activation. Note
355 that because trials containing disfluencies were regressed out of the first-level effects,
356 correlations with Disfluency Rate are capturing activation related to the *propensity* to stutter and
357 not disfluent speech itself. The primary analyses were performed using a strict statistical
358 correction of $p_{FDR} < 0.05$, while the exploratory analyses were performed using an uncorrected
359 alpha level of 0.05.

360

361 *Functional Connectivity Analysis*

362 *Preprocessing and analysis:* Seed-based functional connectivity analyses (SBC) were carried
363 out using the CONN toolbox (Whitfield-Gabrieli & Nieto-Castanon, 2012). The same
364 preprocessed data used for the task activation analysis were used for the functional connectivity
365 analysis. The seeds for this analysis comprised the same “speech production” ROIs used in the
366 exploratory task activation analysis, defined either in *fsaverage* surface (cortical) or MNI volume
367 (subcortical) space. The BOLD time series was averaged within seed ROIs. To include
368 connections between the speech production network and other regions that potentially have a

THE NEURAL CIRCUITRY UNDERLYING THE “RHYTHM EFFECT” IN STUTTERING

369 moderating effect on this network, the target area in this analysis was extended to the whole
370 brain. The target functional volume data were smoothed using an 8 mm full-width half maximum
371 Gaussian smoothing kernel. Following preprocessing, an aCompCor (Behzadi et al., 2007)
372 denoising procedure was used to eliminate extraneous motion, physiological, and artifactual
373 effects from the BOLD signal in each subject. In each seed ROI and every voxel in the smoothed
374 brain volume, denoising was carried out using a linear regression model (Nieto-Castañón, 2020)
375 that included 5 white matter regressors, 5 CSF regressors, 6 subject-motion parameters plus their
376 first-order temporal derivatives, scrubbing regressors to remove the effects of outlier scans (from
377 artifact detection, described above), as well as separate regressors for each run/session (constant
378 effects and first-order linear-trends), task condition (main and first-order derivative terms), and
379 error trials. No band-pass filter was applied in order to preserve high-frequency fluctuations in
380 the residual data.

381 For each participant, a generalized PsychoPhysiological Interaction (gPPI; McLaren et
382 al., 2012) analysis was implemented using a multiple regression model, predicting the signal in
383 each target voxel with three sets of regressors: a) the BOLD time series in a seed ROI,
384 characterizing baseline connectivity between a seed ROI and each target voxel; b) the main
385 effects of each of the task conditions (*normal*, *rhythm*, and *baseline*), characterizing direct
386 functional responses to each task in the target voxel; and c) their seed-time-series-by-task
387 interactions (PPI terms) characterizing the relative changes in functional connectivity strength
388 associated with each task. Second-level random effects analyses were then used to compare these
389 interaction terms within and between groups and conditions, specifically the *Rhythm - Normal*
390 contrast in AWS and ANS and the *Group × Condition* interaction. The same regressors of non-
391 interest used in the task activation analyses were included here as well. For each comparison,

THE NEURAL CIRCUITRY UNDERLYING THE “RHYTHM EFFECT” IN STUTTERING

392 separate analyses were run from the 103 seed ROIs to the whole brain. Within each analysis, a
393 two-step thresholding procedure was used; voxels were thresholded at $p < 0.001$, followed by a
394 cluster-size threshold of $p_{FDR} < 0.05$. To control for family-wise error across the 103 separate
395 seed-to-voxel analyses, a within-comparison Bonferroni correction was applied so that only
396 significant clusters with $p_{FDR} < 0.000485$ ($0.05/103$) survived the threshold.

397

398 **Results**

399 *Behavioral Analysis*

400 Stuttering occurred infrequently over the course of the experiment, with 7 out of 16 AWS
401 producing no disfluencies. There was, however, a significantly lower percentage of disfluent
402 trials in the *rhythm* condition (0.38%) compared to the *normal* condition (1.35%; $W = 42$, $p =$
403 0.023 ; see Figure 3). There was no group \times condition interaction or group main effect on
404 speaking rate but there was a significant main effect of condition with *normal speech* (3.977
405 IVI/sec) produced at a faster rate than *rhythmic speech* (3.460 IVI/sec; $F(1,31) = 37.8$, $p_{FWE} <$
406 0.001). For isochronicity, there was no main effect of group or group \times condition
407 interaction. There was a significant main effect of condition, where subjects had a lower CV-IVI
408 (greater isochronicity) in the *rhythm* condition (0.25) than the *normal* condition (0.13; $F(1,31) =$
409 503.3 , $p_{FWE} < 0.001$).

410

411 *Task Activation fMRI Analysis*

412 The cortical results of the *Normal - Baseline* and *Rhythm - Baseline* contrasts in each
413 group are presented in Supplementary Figure 1. The set of 103 cortical and subcortical ROIs that

THE NEURAL CIRCUITRY UNDERLYING THE “RHYTHM EFFECT” IN STUTTERING

414 were significant in at least one of those contrasts and used for subsequent exploratory analyses is
415 illustrated in Supplementary Figures 2 and 3.

416 For the primary analysis, ANS had greater activation in the *Rhythm* condition compared
417 to the *Normal* condition in left grouped supplementary motor areas (SMAs), posterior superior
418 temporal gyrus (pSTG), ventro-anterior thalamus (VA), and ventro-lateral thalamus (VL), and in
419 right grouped premotor cortex (PMC), caudate nucleus (Caud), and VA ($p_{FDR} < 0.05$, see Table 2
420 and Figure 4). No significant differences were found between conditions in AWS. For the
421 complete exploratory results, see Supplementary Table 1 and Supplementary Figure 4. Notably,
422 eight exploratory ROIs survived an FDR statistical correction: left planum temporale (PT), pre-
423 supplementary motor area (preSMA), superior parietal lobule (SPL), anterior insula (aINS),
424 planum polare (PP), supplementary motor area (SMA), VA, and right ventral premotor cortex
425 (vPMC). For the same exploratory contrast, AWS showed increased activity in left PT, and right
426 ventral inferior frontal gyrus pars opercularis (vIFo) in the *Rhythm* condition, and decreased
427 activation in right anterior dorsal superior temporal sulcus (adSTs) and cerebellar vermis lobule
428 VIIIb. To explore whether the failure of these effects to survive the corrected significance
429 threshold was due to overall greater variability among AWS participants, we averaged *Rhythm* -
430 *Normal* effects across all exploratory ROIs and performed Levene’s test for equality of
431 variances. AWS had significantly larger variance across subjects ($F = 3.42$, $p = 0.019$).

432 For the primary analysis, no significant differences were found between groups for either
433 *Normal* - *Baseline* or *Rhythm* - *Baseline*. In the exploratory analysis, AWS had decreased
434 activation in left anterior frontal operculum (aFO; $p = 0.009$) and the internal portion of the
435 globus pallidus (GPi; $p = 0.047$), as well as midline cerebellar vermis VIIIb ($p = 0.038$), in the
436 *Rhythm* - *Baseline* contrast compared to ANS.

THE NEURAL CIRCUITRY UNDERLYING THE “RHYTHM EFFECT” IN STUTTERING

437 In our primary analysis, no ROIs showed a significant interaction between groups and
438 conditions. In the follow-up exploratory analysis, an interaction was found in five ROIs (see
439 Supplementary Table 2 and Supplementary Figure 5): left PP, aFO, cerebellar lobule VIIIa (Cbm
440 VIIIa), and the external portion of the globus pallidus (GPe), and midline cerebellar vermis VIIIb
441 ($p < 0.05$). In all cases, ANS had increased activation in the *Rhythm* condition compared to
442 *Normal*, while AWS showed no change or a decrease.

443

444 *Brain-Behavior Correlation Analyses*

445 In our primary analysis, no significant correlation was found between SSI-Mod and
446 *Normal - Baseline* or *Rhythm - Baseline* in any ROI when correcting for multiple comparisons.
447 There were, however, significant positive correlations between Disfluency Rate and *Normal -*
448 *Baseline* activation in left VA and VL as well as right VL (Table 3).

449 Exploratory results can be found in Supplementary Table 3. Of note, positive correlations
450 were found between SSI-Mod and activation in bilateral premotor and frontal opercular cortex
451 and negative correlations were found in left anterior auditory cortex. In addition, positive
452 correlations between Disfluency Rate and *Normal - Baseline* were found in right parasyllvian
453 regions and bilateral putamen.

454

455 *Functional Connectivity Analyses*

456 *Within group:* Within the AWS group, seven connections were significantly stronger in
457 the *Rhythm* condition as compared to the *Normal* condition ($p_{FDR} < 0.000485$), all involving the
458 cerebellum (see Table 4 and Figure 5). Both left and right cerebellar lobule VIIIa displayed
459 greater connectivity with clusters in bilateral orbitofrontal cortex (OFC; two distinct clusters with

THE NEURAL CIRCUITRY UNDERLYING THE “RHYTHM EFFECT” IN STUTTERING

460 right cerebellar lobule VIIIa [clusters 3 and 4 in Figure 5], and one cluster with left cerebellar
461 lobule VIIIa straddling the midline [cluster 2]), and right cerebellar lobule VIIb had greater
462 connectivity in an overlapping region of right OFC (cluster 1). Right dentate nucleus showed an
463 increase in connectivity with one cluster covering medial cerebellar lobule VI and Crus I (cluster
464 5), and a second cluster in right lateral cerebellar lobule VI and Crus I (cluster 6). Finally, there
465 was increased connectivity between cerebellar vermis Crus II and a cluster in the superior
466 cerebellum more anteriorly (cluster 7). In all cases, there was either a negative relationship or no
467 relationship during the *Normal* condition, and a positive relationship during the *Rhythm*
468 condition. To determine whether these differences were specific to AWS, a *post hoc* analysis
469 found that these connections did not reach significance in the ANS group, even using an
470 uncorrected alpha level of 0.05. Instead, ANS had different connections that were significantly
471 stronger during *Rhythm* speech compared to *Normal*: between left VA and a cluster in right
472 occipital cortex (OC) and fusiform gyrus (FG); and right preSMA and a cluster at the junction of
473 left SPL, precuneus (PCN), and OC. There was also a decrease in connectivity between left
474 substantia nigra (SN) and a cluster in left OC (see Supplementary Figure 6).

475 *Group × Condition Interaction:* There were four connections that showed a significant
476 interaction between group and speech condition (*Normal* and *Rhythm*; see Figure
477 6). Connections that were lower in the *Rhythm* condition for AWS and greater in this condition
478 for ANS included: right cerebellar lobule V to left medial rolandic cortex and posterior SMA
479 (result cluster labeled 1 in bottom-left panel of Figure 6); left putamen to right aMFG (extending
480 to right medial cortex; cluster 2); and left vPMC to left frontal pole (FP) and anterior middle
481 frontal gyrus (aMFG; cluster 3). A connection that was greater in the *Rhythm* condition for AWS
482 and lesser in this condition for ANS was between right cerebellar lobule V to right cerebellar

THE NEURAL CIRCUITRY UNDERLYING THE “RHYTHM EFFECT” IN STUTTERING

483 lobule Crus I, Crus II, and dentate nucleus (cluster 4). Simple effects from each group and
484 condition are shown in the bottom panel of Figure 6. Based on the results that showed increased
485 connectivity for AWS between different parts of the cerebellum during rhythmic speech, we
486 performed a test comparing average pairwise connectivity among all 21 cerebellar ROIs active
487 during speech. This test revealed that these ROIs show a significant group \times condition
488 interaction ($t = 2.90$, $p = 0.004$), driven by an increase in connectivity for AWS from *Normal* to
489 *Rhythm* ($t = 3.94$, $p < 0.001$) and a non-significant decrease in connectivity for ANS ($t = -1.23$, p
490 $= 0.880$).

491

492 **Discussion**

493 This study aimed to characterize the changes in functional activation and connectivity
494 that occur when adults time their speech to an external metronomic beat and how these changes
495 differ in AWS compared to ANS. Extending previous work, this paradigm was novel in that the
496 metronome was paced at the typical rate of English speech. The rate and rhythmicity of paced
497 speech by AWS was also similar to that of ANS. Consistent with prior literature, AWS produced
498 significantly fewer disfluencies during externally-paced speech than during normal, internally-
499 paced speech (Figure 3). In addition, while ANS exhibited greater activation during rhythmic
500 speech than normal speech in left hemisphere auditory, premotor, and sensory association areas,
501 as well as right hemisphere premotor cortex, AWS did not exhibit any significant differences
502 between the conditions. AWS also had greater functional connectivity during rhythmic speech
503 than normal speech between bilateral inferior cerebellum and orbitofrontal cortex and among all
504 cerebellar speech regions. Finally, functional connections between right cerebellum and medial
505 sensorimotor cortex and between both left vPMC and right putamen and right prefrontal cortex

THE NEURAL CIRCUITRY UNDERLYING THE “RHYTHM EFFECT” IN STUTTERING

506 were significantly modulated by group and condition. The following sections discuss these
507 results in relation to prior behavioral and neuroimaging literature.

508

509 *A Compensatory Role for the Cerebellum in AWS*

510 The role of the cerebellum for mediating speech timing is well-known (see Ackermann,
511 2008 for a review), and damage to this structure can lead to “scanning speech,” where syllables
512 are evenly paced (Duffy, 2013). Previous work posits that when the basal-ganglia-SMA
513 “internal” timing system is impaired in AWS, the cerebellum, along with lateral cortical
514 premotor structures, forms part of an “external” timing system that is recruited (Alm, 2004;
515 Etchell et al., 2014). In support of this, numerous fMRI and PET studies demonstrate cerebellar
516 overactivation and hyper-connectivity during normal speech production in AWS (e.g., Brown et
517 al., 2005; Chang et al., 2009; Ingham et al., 2012; Lu, Peng, et al., 2010; Lu et al., 2012; Watkins
518 et al., 2007) that is reduced following therapy (De Nil et al., 2001; Lu et al., 2012; Neumann et
519 al., 2003; Toyomura et al., 2015), a potential indication of an organic attempt at compensation.
520 In the present study, the increased connectivity among speech-related regions of the cerebellum
521 along with increased fluency during the rhythm condition may thus reflect similar neural
522 processes.

523 It should be noted that this functional connectivity likely does not necessarily reflect
524 direct structural connectivity between a seed and target region. Except in the case of connectivity
525 between the cerebellar cortex and the dentate nucleus, which are structurally connected, viral
526 tracing studies have found that each part of the cerebellar cortex forms closed-loop circuits with
527 areas of cerebral cortex (Strick et al., 2009), meaning that different parts of cerebellar cortex do
528 not communicate directly. Nonetheless, as suggested by (Bernard et al., 2013), we interpret the

THE NEURAL CIRCUITRY UNDERLYING THE “RHYTHM EFFECT” IN STUTTERING

529 result of increased “within-cerebellar” connectivity as reflecting an increase in synchrony among
530 multiple cerebro-cerebellar loops. Thus, in AWS, areas of cerebral cortex may simultaneously
531 impinge on distinct areas of cerebellum to utilize the cerebellum’s temporal processing
532 capabilities to ensure accurate speech timing during the *rhythm* condition.

533 The orbitofrontal cortex has also been shown to play a role in increasing fluency.
534 Previous work on the OFC in AWS have shown greater OFC activation during speech in more
535 fluent speakers (Kell et al., 2009), greater OFC activity following therapy for AWS (Kell et al.,
536 2009), and increased activation in adults who spontaneously recovered from stuttering during
537 adulthood in the left OFC compared to both persistent AWS and controls (Kell et al., 2009). The
538 current study did not show greater activation in the OFC, but did show increased connectivity
539 with the cerebellum during rhythmic speech. Previous studies have also found a relationship
540 between increased functional connectivity between the cerebellum and the OFC and decreased
541 stuttering severity in AWS (Sitek et al., 2016) and in adults who spontaneously recovered from
542 stuttering during adulthood compared to ANS (Kell et al., 2018). Thus, increased connectivity
543 between the cerebellum and OFC may underpin successful long-term compensatory behavior
544 (i.e. fluency), which is induced by the rhythm condition in the current study.

545 There were also cerebellar connections that showed significant interactions between
546 groups and conditions whereby the rhythm condition had the opposite effect on connectivity in
547 the two groups. The AWS group had increased connectivity between right cerebellar lobule V
548 and another cluster in posterior cerebellum, while the ANS had decreased connectivity. This
549 increase in the AWS supports the earlier argument that increased connectivity within the
550 cerebellum may reflect a compensatory mechanism. The AWS group also had decreased
551 connectivity between the right cerebellum lobule V and left medial sensorimotor cortex and

THE NEURAL CIRCUITRY UNDERLYING THE “RHYTHM EFFECT” IN STUTTERING

552 SMA, while the ANS group had increased connectivity between these areas. This may reflect
553 that AWS have positive connectivity between the cerebellum (“external”) and medial premotor
554 (“internal”) areas in the normal condition to compensate for the impaired “internal” basal-ganglia
555 timing system. This connection is decreased in the rhythm condition because the AWS no longer
556 attempt to use the medial structures. Conversely, ANS may have increased connectivity between
557 these regions in the rhythm condition because the internal system is both working properly and is
558 being used to a greater extent as seen in the task activation results. Together, all of these results
559 support the theory that in AWS, an “external” timing system mediated by the cerebellum plays
560 an increased role in speech production during externally-timed speech and can lead to increased
561 fluency.

562

563 *Increased Prefrontal Mediation During Rhythmic Speech*

564 The AWS group also had decreased functional connections between right aMFG and both
565 right vPMC and right putamen during the rhythm condition, whereas the ANS had increased
566 connectivity. The right aMFG, a portion of dorsolateral prefrontal cortex, has been previously
567 implicated in high-level cognitive tasks that require holding multiple pieces of information in
568 memory (Barbey et al., 2013; Wager & Smith, 2003), including reframing emotional situations
569 (Falquez et al., 2014; Ochsner et al., 2012). In the context of stuttering, it is well known that
570 people who stutter will often monitor their upcoming speech in order to anticipate and potentially
571 correct disfluencies (Garcia-Barrera & Davidow, 2015; Jackson et al., 2015). However, after
572 noticing how speaking along with a metronome improves fluency, they may be less likely to
573 continuously monitor their speech to the same extent. Therefore, decreased connectivity between
574 right aMFG and left vPMC, an area hypothesized to encode speech motor programs (Guenther,

THE NEURAL CIRCUITRY UNDERLYING THE “RHYTHM EFFECT” IN STUTTERING

575 2016), in the rhythm condition may reflect this decreased monitoring of upcoming speech. As
576 connections between lateral prefrontal cortex and basal ganglia structures mediate attention-
577 shifting (Morris et al., 2016), decreased monitoring may also lead to decreased connectivity
578 between right aMFG and right putamen. ANS, on the other hand, may exhibit an increase in
579 connectivity between these regions because there is no fluency advantage to rhythmic speech and
580 may require more monitoring to speak rhythmically. This conscious shift in attention may be
581 mediated by increased connectivity between right putamen and right aMFG in ANS (Morris et
582 al., 2016). Thus, the interaction found between group and condition in functional connections
583 between speech planning and sequencing areas and right aMFG may be reflective of different
584 changes in attentional demands between groups.

585

586 *Changes in Activation due to Rhythmically-Timed Speech*

587 Comparing neural activation between rhythmic and normal speech showed that ANS had
588 greater activation during rhythmic speech than normal speech in left hemisphere auditory,
589 premotor, and sensory association areas, as well as right hemisphere ventral premotor
590 cortex. Activation in left auditory associative cortex (PT, PP) and right ventral premotor cortex
591 (vPMC) may be related to increased reliance on auditory feedback control during this novel
592 speech condition. Previous studies have shown that auditory feedback errors lead to increased
593 activation in posterior auditory areas (Hashimoto & Sakai, 2003; Parkinson et al., 2012; Takaso
594 et al., 2010; Tourville et al., 2008), and greater activation in right vPMC is thought to generate
595 corrective responses to sensory errors in response to this altered sensory feedback
596 (Golfopoulos et al., 2011; Hashimoto & Sakai, 2003; Tourville et al., 2008). Alternatively, left
597 PT has been described as an auditory-motor interface (Hickok et al., 2003); therefore increased

THE NEURAL CIRCUITRY UNDERLYING THE “RHYTHM EFFECT” IN STUTTERING

598 activation in left PT may be indicative of the need to hold the rhythmic auditory stimulus in
599 working memory and translate it into a motoric response in the rhythm condition of the current
600 study. This is supported by increased activity (found in the exploratory analysis) in left anterior
601 insula and superior parietal lobule, additional regions commonly recruited in working memory
602 tasks (Rottschy et al., 2012).

603 There was also increased activation during rhythmic speech in areas thought to be
604 involved in speech planning and sequencing (left SMA, pre-SMA, caudate and VA; Bohland et
605 al., 2010; Civier et al., 2013; Guenther, 2016), articulatory planning of complex sequences (left
606 aINS; (Ackermann & Riecker, 2010; Bohland & Guenther, 2006; Shuster & Lemieux, 2005),
607 producing complex motor sequences (left SPL; Haslinger et al., 2002; Heim et al., 2012),
608 producing untrained sequences (left SPL; Jenkins et al., 1994; Segawa et al., 2015), and
609 attending to stimulus timing (left SPL; Coull, 2004). The rhythm condition requires participants
610 to produce speech in an unfamiliar way. This change in their speech production results in speech
611 becoming less automatic, and may require greater recruitment in these areas for timing the
612 sequence of syllables (Alario et al., 2006; Bohland & Guenther, 2006; Schubotz & von Cramon,
613 2001). Bengtsson et al. (2004, 2005) found that for both finger tapping and simple repetition of
614 “pa,” more complex timing led to increased activation in SMA and preSMA compared to simple
615 patterns. The increased need to implement a timing pattern recruited these same structures that
616 mediate temporal sequencing.

617 Unlike previous studies (Braun et al., 1997; Stager et al., 2003; Toyomura et al., 2011,
618 2015), AWS did not exhibit significantly increased activation in the *rhythm* condition compared
619 to the *normal* condition. The most consistent finding from these studies was that both
620 groups showed increased activation in bilateral auditory regions during rhythmic speech and that

THE NEURAL CIRCUITRY UNDERLYING THE “RHYTHM EFFECT” IN STUTTERING

621 AWS showed greater increases in the basal ganglia. In the present study, the lack of clear
622 between-condition effects within the AWS or between the AWS and ANS group may be due to
623 more individual variability for AWS than ANS for this contrast. Future work is needed to
624 determine whether this within-group variability is driving the null findings in the AWS group.
625 Furthermore, Toyomura et al. (2011) found that while areas of the basal ganglia, left precentral
626 gyrus, left SMA, left IFG, and left insula were less active in AWS during normal speech, activity
627 in these areas increased to the level of ANS during rhythmic speech. These results suggested that
628 rhythmic speech had a “normalizing” effect on activity in these regions, which differs with the
629 present results.

630 There are methodological differences between the current work and similar studies that
631 also could have impacted the results. In the current study, the rhythmic stimulus was presented
632 prior to speaking regardless of the condition, unlike previous work in which the participant heard
633 the stimulus while speaking and only during the rhythmic condition (Toyomura et al. 2011).
634 Thus, group effects reported by Toyomura and colleagues (2011) may reflect differences in
635 processing the auditory pacing stimulus in addition to differences in speech motor processes.
636 Second, our study sought to examine the rhythm effect when speech was produced at a
637 conversational speaking rate. Previous studies used a metronome set at 92 - 100 beats per
638 minute, considerably slower than the mean conversational rate in English (228 - 372 syllables
639 per minute; Davidow, 2014; Pellegrino et al., 2011) and the rate observed in our study
640 (approximately 207 syllables per minute). While Toyomura et al. (2011, 2015) instructed
641 participants to speak at a similar rate during the normal condition (when previous studies had
642 not), the slower tempo overall may have led to increased auditory feedback processing. This
643 could have modified the mechanisms by which ANS and AWS controlled their speech timing.

THE NEURAL CIRCUITRY UNDERLYING THE “RHYTHM EFFECT” IN STUTTERING

644 Finally, only one of the previous studies accounted for disfluencies during the task in their
645 imaging analysis (Stager et al., 2003), despite significant correlations with brain activation
646 (Braun et al., 1997). However, given the small number of disfluencies in this and previous
647 studies, this effect may have had a limited impact on the results.

648

649 *Correlation Between Activation and Severity*

650 The primary analysis found significant positive correlations between Disfluency Rate and
651 activation in the *Normal-Baseline* contrast in left VA thalamus and bilateral VL thalamus. These
652 nuclei are part of both the cortico-cerebellar and cortico-basal ganglia motor loops, and are
653 structurally connected with premotor and primary motor areas (Barbas et al., 2013). As relays
654 between subcortical structures and the cortex, increased activation for participants with a higher
655 disfluency rate during the task may reflect greater reliance upon these modulatory pathways
656 during speech. It is also worth noting that with an exploratory threshold ($p < 0.05$, uncorrected),
657 some ROIs follow similar patterns to previous literature. Higher SSI-Mod scores were associated
658 with weaker activation in left auditory areas. This correlation has been shown before (Fox et al.,
659 2000) and there are numerous reports of atypical activity and/or morphology in left auditory
660 cortex in AWS (e.g. Belyk et al., 2015; Chang et al., 2009; De Nil et al., 2000, 2008; Fox et al.,
661 1996; Stager et al., 2003; Van Borsel et al., 2003). Similarly, the propensity to stutter during the
662 task, measured by Disfluency Rate, is associated with greater cortical activation in largely right
663 hemisphere regions, and bilateral subcortical activation at uncorrected thresholds. The right-
664 lateralized cortical associations in the present study may reflect increased compensatory activity
665 in AWS (as in Braun et al., 1997; Cai et al., 2014; Kell et al., 2009; Preibisch et al., 2003;
666 Salmelin et al., 2000). This is supported by the fact that fluency-inducing therapy lead to more

THE NEURAL CIRCUITRY UNDERLYING THE “RHYTHM EFFECT” IN STUTTERING

667 left-lateralized activation (De Nil et al., 2003; Neumann et al., 2003, 2005), similar to that of
668 neurotypical speakers. It should be noted that due to the low number of disfluencies exhibited
669 during the task, determining a clear relationship between stuttering severity and activation may
670 not have been possible.

671

672 *Limitations*

673 Despite training in a prior session and feedback immediately prior to scanning,
674 participants’ *rhythmic* speech productions were significantly slower than their *normal* speech
675 productions. Since rate reduction is another method that reduces disfluencies in PWS (Andrews
676 et al., 1982), this potentially could have led to the changes in both fluency and brain activation
677 found herein. This same issue was reported in one previous neuroimaging study of the
678 metronome-timed speech effect (Toyomura et al., 2011). As previously mentioned, the effect on
679 rhythmic speech on fluency occurs even at high speaking rates (Davidow, 2014). Additionally,
680 studies examining the effect of speaking rate on brain activation have found positive correlations
681 with activation in sensorimotor cortex, SMA, insula, thalamus, and cerebellum (Fox et al., 2000;
682 Riecker et al., 2006). This is the opposite effect of what we would expect given that increased
683 activation was found (in ANS) during the slower *rhythmic* condition. While not conclusive, this
684 evidence mitigates the concern that a decreased speaking rate accounted for neural changes
685 found in this study.

686 In addition, the current results are not consistent with a recent meta-analysis examining
687 activation differences between AWS and ANS (Belyk et al., 2015, 2017) which found that AWS
688 consistently had overactivation in right hemisphere cortical structures, and underactivation in left
689 hemisphere structures, especially in motor and premotor areas. However, the present study’s

THE NEURAL CIRCUITRY UNDERLYING THE “RHYTHM EFFECT” IN STUTTERING

690 exploratory analysis suggested that AWS had decreased activation in left frontal operculum
691 during the rhythmic condition as compared to the ANS group. Previous work has shown gray
692 matter and white matter anomalies in and near left IFG (Beal et al., 2013, 2015; Chang et al.,
693 2008, 2011; Kell et al., 2009; Lu et al., 2012), which may be related to this under-activation.
694 Based on the exploratory nature of these findings, future work as well as meta-analytic testing is
695 needed to determine whether these are true population differences.

696

697 **Conclusion**

698 In this study, we examined brain activation patterns that co-occur with the introduction of
699 an external pacing stimulus. We found that AWS showed an overall decrease in disfluencies
700 during this condition, as well as functional connectivity changes between the cerebellum,
701 prefrontal cortex, and other regions of the speech production network. Involvement of these
702 structures suggests that rhythmic speech activates compensatory timing systems and potentially
703 enhances top-down feedback control and attentional systems. This study provides greater insight
704 into the network of brain areas that either support (or respond to) fluency in relation to the
705 rhythm effect and its correspondence to longer-term fluency provided through natural
706 compensation or therapy. It is our hope that in conjunction with the large body of work already
707 published on fluency-enhancing techniques and future studies with more focused analyses, the
708 field will come to a better understanding of the pathophysiology of stuttering and fluency, and
709 that this information will be used to provide more targeted treatments and, ultimately, improve
710 quality of life for those who stutter.

711

712 **Acknowledgements:**

THE NEURAL CIRCUITRY UNDERLYING THE “RHYTHM EFFECT” IN STUTTERING

713 The research reported here was supported by grants from the National Institute of Health (R01
714 DC007683, T32 DC013017, P41 RR14075) and the National Science Foundation (NSF
715 1625552). We are grateful to Diane Constantino, Barbara Holland, Matthias Heyne, Megan
716 Thompson, Elaine Kearney, Julianne Leber, and Erin Archibald for assistance with subject
717 recruitment and data collection and Ina Jessen, Mona Tong and Brittany Steinfeld for their help
718 with behavioral data analysis. This work benefited from helpful discussions with, or comments
719 from, other members of the Boston University Speech Lab.

THE NEURAL CIRCUITRY UNDERLYING THE “RHYTHM EFFECT” IN STUTTERING

720 **References**

- 721 Ackermann, H. (2008). Cerebellar contributions to speech production and speech perception:
722 Psycholinguistic and neurobiological perspectives. *Trends in Neurosciences*, *31*(6), 265–
723 272. <https://doi.org/10.1016/j.tins.2008.02.011>
- 724 Ackermann, H., & Riecker, A. (2010). The contribution(s) of the insula to speech production: A
725 review of the clinical and functional imaging literature. *Brain Structure and Function*,
726 *214*(5–6), 419–433. <https://doi.org/10.1007/s00429-010-0257-x>
- 727 Alario, F.-X., Chainay, H., Lehericy, S., & Cohen, L. (2006). The role of the supplementary
728 motor area (SMA) in word production. *Brain Research*, *1076*(1), 129–143.
729 <https://doi.org/10.1016/j.brainres.2005.11.104>
- 730 Alm, P. A. (2004). Stuttering and the basal ganglia circuits: A critical review of possible
731 relations. *Journal of Communication Disorders*, *37*(4), 325–369.
732 <https://doi.org/10.1016/j.jcomdis.2004.03.001>
- 733 Andersson, J. L. R., Hutton, C., Ashburner, J., Turner, R., & Friston, K. (2001). Modeling
734 Geometric Deformations in EPI Time Series. *NeuroImage*, *13*(5), 903–919.
735 <https://doi.org/10.1006/nimg.2001.0746>
- 736 Andrews, G., Howie, P. M., Dozsa, M., & Guitar, B. E. (1982). Stuttering: Speech pattern
737 characteristics under fluency-inducing conditions. *Journal of Speech and Hearing*
738 *Research*, *25*(2), 208–216.
- 739 Ashburner, J., & Friston, K. J. (2005). Unified segmentation. *NeuroImage*, *26*(3), 839–851.
740 <https://doi.org/10.1016/j.neuroimage.2005.02.018>
- 741 Azrin, N., Jones, R. J., & Flye, B. (1968). A synchronization effect and its application to
742 stuttering by a portable apparatus¹. *Journal of Applied Behavior Analysis*, *1*(4), 283–295.
743 <https://doi.org/10.1901/jaba.1968.1-283>

THE NEURAL CIRCUITRY UNDERLYING THE “RHYTHM EFFECT” IN STUTTERING

- 744 Barbas, H., García-Cabezas, M. Á., & Zikopoulos, B. (2013). Frontal-thalamic circuits
745 associated with language. *Brain and Language*, *126*(1), 49–61.
746 <https://doi.org/10.1016/j.bandl.2012.10.001>
- 747 Barber, V. (1940). Studies in the Psychology of Stuttering, XVI: Rhythm as a Distraction in
748 Stuttering. *Journal of Speech Disorders*, *5*(1), 29–42.
749 <https://doi.org/10.1044/jshd.0501.29>
- 750 Barbey, A. K., Koenigs, M., & Grafman, J. (2013). Dorsolateral prefrontal contributions to
751 human working memory. *Cortex*, *49*(5), 1195–1205.
752 <https://doi.org/10.1016/j.cortex.2012.05.022>
- 753 Beal, D. S., Gracco, V. L., Brettschneider, J., Kroll, R. M., & De Nil, L. F. (2013). A voxel-
754 based morphometry (VBM) analysis of regional grey and white matter volume
755 abnormalities within the speech production network of children who stutter. *Cortex*,
756 *49*(8), 2151–2161. <https://doi.org/10.1016/j.cortex.2012.08.013>
- 757 Beal, D. S., Lerch, J. P., Cameron, B., Henderson, R., Gracco, V. L., & De Nil, L. F. (2015). The
758 trajectory of gray matter development in Broca’s area is abnormal in people who
759 stutter. *Frontiers in Human Neuroscience*, *9*. <https://doi.org/10.3389/fnhum.2015.00089>
- 760 Behzadi, Y., Restom, K., Liau, J., & Liu, T. T. (2007). A component based noise correction
761 method (CompCor) for BOLD and perfusion based fMRI. *NeuroImage*, *37*(1), 90–101.
762 <https://doi.org/10.1016/j.neuroimage.2007.04.042>
- 763 Belin, P., Zatorre, R. J., Hoge, R., Evans, A. C., & Pike, B. (1999). Event-Related fMRI of the
764 Auditory Cortex. *NeuroImage*, *10*(4), 417–429. <https://doi.org/10.1006/nimg.1999.0480>

THE NEURAL CIRCUITRY UNDERLYING THE “RHYTHM EFFECT” IN STUTTERING

- 765 Belyk, M., Kraft, S. J., & Brown, S. (2015). Stuttering as a trait or state—An ALE meta-analysis
766 of neuroimaging studies. *European Journal of Neuroscience*, *41*(2), 275–284.
767 <https://doi.org/10.1111/ejn.12765>
- 768 Belyk, M., Kraft, S. J., & Brown, S. (2017). Stuttering as a trait or a state revisited: Motor system
769 involvement in persistent developmental stuttering. *European Journal of Neuroscience*,
770 *45*(4), 622–624. <https://doi.org/10.1111/ejn.13512>
- 771 Bengtsson, S. L., Ehrsson, H. H., Forssberg, H., & Ullen, F. (2004). Dissociating brain regions
772 controlling the temporal and ordinal structure of learned movement sequences. *European*
773 *Journal of Neuroscience*, *19*(9), 2591–2602. [https://doi.org/10.1111/j.0953-](https://doi.org/10.1111/j.0953-816X.2004.03269.x)
774 [816X.2004.03269.x](https://doi.org/10.1111/j.0953-816X.2004.03269.x)
- 775 Bengtsson, S. L., Ehrsson, H. H., Forssberg, H., & Ullén, F. (2005). Effector-independent
776 voluntary timing: Behavioural and neuroimaging evidence. *European Journal of*
777 *Neuroscience*, *22*(12), 3255–3265. <https://doi.org/10.1111/j.1460-9568.2005.04517.x>
- 778 Benjamini, Y., & Hochberg, Y. (1995). Controlling the False Discovery Rate: A Practical and
779 Powerful Approach to Multiple Testing. *Journal of the Royal Statistical Society: Series B*
780 *(Methodological)*, *57*(1), 289–300. <https://doi.org/10.1111/j.2517-6161.1995.tb02031.x>
- 781 Bernard, J. A., Peltier, S. J., Wiggins, J. L., Jaeggi, S. M., Buschkuhl, M., Fling, B. W., Kwak,
782 Y., Jonides, J., Monk, C. S., & Seidler, R. D. (2013). Disrupted cortico-cerebellar
783 connectivity in older adults. *NeuroImage*, *83*, 103–119.
784 <https://doi.org/10.1016/j.neuroimage.2013.06.042>
- 785 Bohland, J. W., Bullock, D., & Guenther, F. H. (2010). Neural representations and mechanisms
786 for the performance of simple speech sequences. *Journal of Cognitive Neuroscience*,
787 *22*(7), 1504–1529.

THE NEURAL CIRCUITRY UNDERLYING THE “RHYTHM EFFECT” IN STUTTERING

- 788 Bohland, J. W., & Guenther, F. H. (2006). An fMRI investigation of syllable sequence
789 production. *NeuroImage*, 32(2), 821–841.
790 <https://doi.org/10.1016/j.neuroimage.2006.04.173>
- 791 Braun, A. R., Varga, M., Stager, S., Schulz, G., Selbie, S., Maisog, J. M., Carson, R. E., &
792 Ludlow, C. L. (1997). Altered patterns of cerebral activity during speech and language
793 production in developmental stuttering. An H2 (15) O positron emission tomography
794 study. *Brain*, 120(5), 761–784.
- 795 Brown, S., Ingham, R. J., Ingham, J. C., Laird, A. R., & Fox, P. T. (2005). Stuttered and fluent
796 speech production: An ALE meta-analysis of functional neuroimaging studies. *Human*
797 *Brain Mapping*, 25(1), 105–117. <https://doi.org/10.1002/hbm.20140>
- 798 Cai, S., Tourville, J. A., Beal, D. S., Perkell, J. S., Guenther, F. H., & Ghosh, S. S. (2014).
799 Diffusion imaging of cerebral white matter in persons who stutter: Evidence for network-
800 level anomalies. *Frontiers in Human Neuroscience*, 8.
801 <https://doi.org/10.3389/fnhum.2014.00054>
- 802 Chang, S.-E., Erickson, K. I., Ambrose, N. G., Hasegawa-Johnson, M. A., & Ludlow, C. L.
803 (2008). Brain anatomy differences in childhood stuttering. *NeuroImage*, 39(3), 1333–
804 1344. <https://doi.org/10.1016/j.neuroimage.2007.09.067>
- 805 Chang, S.-E., Horwitz, B., Ostuni, J., Reynolds, R., & Ludlow, C. L. (2011). Evidence of Left
806 Inferior Frontal–Premotor Structural and Functional Connectivity Deficits in Adults Who
807 Stutter. *Cerebral Cortex*, 21(11), 2507–2518. <https://doi.org/10.1093/cercor/bhr028>
- 808 Chang, S.-E., Kenney, M. K., Loucks, T. M. J., & Ludlow, C. L. (2009). Brain activation
809 abnormalities during speech and non-speech in stuttering speakers. *NeuroImage*, 46(1),
810 201–212. <https://doi.org/10.1016/j.neuroimage.2009.01.066>

THE NEURAL CIRCUITRY UNDERLYING THE “RHYTHM EFFECT” IN STUTTERING

- 811 Chang, S.-E., & Zhu, D. C. (2013). Neural network connectivity differences in children who
812 stutter. *Brain*, *136*(12), 3709–3726. <https://doi.org/10.1093/brain/awt275>
- 813 Chauvigné, L. A. S., Gitau, K. M., & Brown, S. (2014). The neural basis of audiomotor
814 entrainment: An ALE meta-analysis. *Frontiers in Human Neuroscience*, *8*.
815 <https://doi.org/10.3389/fnhum.2014.00776>
- 816 Civier, O., Bullock, D., Max, L., & Guenther, F. H. (2013). Computational modeling of
817 stuttering caused by impairments in a basal ganglia thalamo-cortical circuit involved in
818 syllable selection and initiation. *Brain and Language*, *126*(3), 263–278.
819 <https://doi.org/10.1016/j.bandl.2013.05.016>
- 820 Coull, J. T. (2004). fMRI studies of temporal attention: Allocating attention within, or towards,
821 time. *Cognitive Brain Research*, *21*(2), 216–226.
822 <https://doi.org/10.1016/j.cogbrainres.2004.02.011>
- 823 Craig, A., Blumgart, E., & Tran, Y. (2009). The impact of stuttering on the quality of life in
824 adults who stutter. *Journal of Fluency Disorders*, *34*(2), 61–71.
825 <https://doi.org/10.1016/j.jfludis.2009.05.002>
- 826 Craig, A., & Tran, Y. (2006). Fear of speaking: Chronic anxiety and stammering. *Advances in*
827 *Psychiatric Treatment*, *12*(1), 63–68. <https://doi.org/10.1192/apt.12.1.63>
- 828 Craig, A., & Tran, Y. (2014). Trait and social anxiety in adults with chronic stuttering:
829 Conclusions following meta-analysis. *Journal of Fluency Disorders*, *40*, 35–43.
830 <https://doi.org/10.1016/j.jfludis.2014.01.001>
- 831 Davidow, J. H. (2014). Systematic studies of modified vocalization: The effect of speech rate on
832 speech production measures during metronome-paced speech in persons who stutter:
833 Speech rate and speech production measures during metronome-paced speech in PWS.

THE NEURAL CIRCUITRY UNDERLYING THE “RHYTHM EFFECT” IN STUTTERING

- 834 *International Journal of Language & Communication Disorders*, 49(1), 100–112.
835 <https://doi.org/10.1111/1460-6984.12050>
- 836 De Nil, L. F., Kroll, R. M., & Houle, S. (2001). Functional neuroimaging of cerebellar activation
837 during single word reading and verb generation in stuttering and nonstuttering adults.
838 *Neuroscience Letters*, 302(2–3), 77–80. [https://doi.org/10.1016/s0304-3940\(01\)01671-8](https://doi.org/10.1016/s0304-3940(01)01671-8)
- 839 De Nil, Luc F., Beal, D. S., Lafaille, S. J., Kroll, R. M., Crawley, A. P., & Gracco, V. L. (2008).
840 The effects of simulated stuttering and prolonged speech on the neural activation patterns
841 of stuttering and nonstuttering adults. *Brain and Language*, 107(2), 114–123.
842 <https://doi.org/10.1016/j.bandl.2008.07.003>
- 843 De Nil, Luc F., Kroll, R. M., Kapur, S., & Houle, S. (2000). A Positron Emission Tomography
844 Study of Silent and Oral Single Word Reading in Stuttering and Nonstuttering Adults.
845 *Journal of Speech, Language, and Hearing Research*, 43(4), 1038–1053.
846 <https://doi.org/10.1044/jslhr.4304.1038>
- 847 De Nil, Luc F., Kroll, R. M., Lafaille, S. J., & Houle, S. (2003). A positron emission tomography
848 study of short- and long-term treatment effects on functional brain activation in adults
849 who stutter. *Journal of Fluency Disorders*, 28(4), 357–380.
850 <https://doi.org/10.1016/j.jfludis.2003.07.002>
- 851 Diedrichsen, J. (2006). A spatially unbiased atlas template of the human cerebellum.
852 *NeuroImage*, 33(1), 127–138. <https://doi.org/10.1016/j.neuroimage.2006.05.056>
- 853 Diedrichsen, J., Balsters, J. H., Flavell, J., Cussans, E., & Ramnani, N. (2009). A probabilistic
854 MR atlas of the human cerebellum. *NeuroImage*, 46(1), 39–46.
855 <https://doi.org/10.1016/j.neuroimage.2009.01.045>

THE NEURAL CIRCUITRY UNDERLYING THE “RHYTHM EFFECT” IN STUTTERING

- 856 Diedrichsen, J., Maderwald, S., Küper, M., Thürling, M., Rabe, K., Gizewski, E. R., Ladd, M. E.,
857 & Timmann, D. (2011). Imaging the deep cerebellar nuclei: A probabilistic atlas and
858 normalization procedure. *NeuroImage*, *54*(3), 1786–1794.
859 <https://doi.org/10.1016/j.neuroimage.2010.10.035>
- 860 Duffy, J. R. (2013). *Motor speech disorders: Substrates, differential diagnosis, and management*
861 (Third edition). Elsevier.
- 862 Eden, G. F., Joseph, J. E., Brown, H. E., Brown, C. P., & Zeffiro, T. A. (1999). Utilizing
863 hemodynamic delay and dispersion to detect fMRI signal change without auditory
864 interference: The behavior interleaved gradients technique. *Magnetic Resonance in*
865 *Medicine*, *41*(1), 13–20. [https://doi.org/10.1002/\(SICI\)1522-2594\(199901\)41:1<13::AID-](https://doi.org/10.1002/(SICI)1522-2594(199901)41:1<13::AID-MRM4>3.0.CO;2-T)
866 [MRM4>3.0.CO;2-T](https://doi.org/10.1002/(SICI)1522-2594(199901)41:1<13::AID-MRM4>3.0.CO;2-T)
- 867 Etchell, A. C., Civier, O., Ballard, K. J., & Sowman, P. F. (2018). A systematic literature review
868 of neuroimaging research on developmental stuttering between 1995 and 2016. *Journal*
869 *of Fluency Disorders*, *55*, 6–45. <https://doi.org/10.1016/j.jfludis.2017.03.007>
- 870 Etchell, A. C., Johnson, B. W., & Sowman, P. F. (2014). Behavioral and multimodal
871 neuroimaging evidence for a deficit in brain timing networks in stuttering: A hypothesis
872 and theory. *Frontiers in Human Neuroscience*, *8*.
873 <https://doi.org/10.3389/fnhum.2014.00467>
- 874 Falquez, R., Couto, B., Ibanez, A., Freitag, M. T., Berger, M., Arens, E. A., Lang, S., & Barnow,
875 S. (2014). Detaching from the negative by reappraisal: The role of right superior frontal
876 gyrus (BA9/32). *Frontiers in Behavioral Neuroscience*, *8*.
877 <https://doi.org/10.3389/fnbeh.2014.00165>

THE NEURAL CIRCUITRY UNDERLYING THE “RHYTHM EFFECT” IN STUTTERING

- 878 Fischl, B., Sereno, M. I., & Dale, A. M. (1999). Cortical Surface-Based Analysis. *NeuroImage*,
879 9(2), 195–207. <https://doi.org/10.1006/nimg.1998.0396>
- 880 Fox, P. T., Ingham, R. J., Ingham, J. C., Hirsch, T. B., Downs, J. H., Martin, C., Jerabek, P.,
881 Glass, T., & Lancaster, J. L. (1996). A PET study of the neural systems of stuttering.
882 *Nature*, 382(6587), 158–162. <https://doi.org/10.1038/382158a0>
- 883 Fox, P. T., Ingham, R. J., Ingham, J. C., Zamarripa, F., Xiong, J. H., & Lancaster, J. L. (2000).
884 Brain correlates of stuttering and syllable production. A PET performance-correlation
885 analysis. *Brain: A Journal of Neurology*, 123 (Pt 10), 1985–2004.
- 886 Garcia-Barrera, M. A., & Davidow, J. H. (2015). Anticipation in stuttering: A theoretical model
887 of the nature of stutter prediction. *Journal of Fluency Disorders*, 44, 1–15.
888 <https://doi.org/10.1016/j.jfludis.2015.03.002>
- 889 Garnett, E. O., Chow, H. M., Nieto-Castañón, A., Tourville, J. A., Guenther, F. H., & Chang, S.
890 E. (2018). Anomalous morphology in left hemisphere motor and premotor cortex of
891 children who stutter. *Brain*, 141(9), 2670–2684. <https://doi.org/10.1093/brain/awy199>
- 892 Giraud, A. (2008). Severity of dysfluency correlates with basal ganglia activity in persistent
893 developmental stuttering. *Brain and Language*, 104(2), 190–199.
894 <https://doi.org/10.1016/j.bandl.2007.04.005>
- 895 Golfopoulos, E., Tourville, J. A., Bohland, J. W., Ghosh, S. S., Nieto-Castanon, A., &
896 Guenther, F. H. (2011). FMRI investigation of unexpected somatosensory feedback
897 perturbation during speech. *NeuroImage*, 55(3), 1324–1338.
898 <https://doi.org/10.1016/j.neuroimage.2010.12.065>
- 899 Gracco, V. L., Tremblay, P., & Pike, B. (2005). Imaging speech production using fMRI.
900 *NeuroImage*, 26(1), 294–301. <https://doi.org/10.1016/j.neuroimage.2005.01.033>

THE NEURAL CIRCUITRY UNDERLYING THE “RHYTHM EFFECT” IN STUTTERING

- 901 Guenther, F. H. (2016). *Neural control of speech*. MIT Press.
- 902 Guitar, B. (2014). *Stuttering: An integrated approach to its nature and treatment* (4th ed).
903 Wolters Kluwer Health/Lippincott Williams & Wilkins.
- 904 Hall, D. A., Haggard, M. P., Akeroyd, M. A., Palmer, A. R., Summerfield, A. Q., Elliott, M. R.,
905 Gurney, E. M., & Bowtell, R. W. (1999). “Sparse” temporal sampling in auditory fMRI.
906 *Human Brain Mapping*, 7(3), 213–223. [https://doi.org/10.1002/\(sici\)1097-](https://doi.org/10.1002/(sici)1097-0193(1999)7:3<213::aid-hbm5>3.0.co;2-n)
907 [0193\(1999\)7:3<213::aid-hbm5>3.0.co;2-n](https://doi.org/10.1002/(sici)1097-0193(1999)7:3<213::aid-hbm5>3.0.co;2-n)
- 908 Hanna, R., & Morris, S. (1977). Stuttering, Speech Rate, and the Metronome Effect. *Perceptual*
909 *and Motor Skills*, 44(2), 452–454. <https://doi.org/10.2466/pms.1977.44.2.452>
- 910 Hashimoto, Y., & Sakai, K. L. (2003). Brain activations during conscious self-monitoring of
911 speech production with delayed auditory feedback: An fMRI study. *Human Brain*
912 *Mapping*, 20(1), 22–28. <https://doi.org/10.1002/hbm.10119>
- 913 Haslinger, B., Erhard, P., Weilke, F., Ceballos-Baumann, A. O., Bartenstein, P., Gräfin von
914 Einsiedel, H., Schwaiger, M., Conrad, B., & Boecker, H. (2002). The role of lateral
915 premotor–cerebellar–parietal circuits in motor sequence control: A parametric fMRI
916 study. *Cognitive Brain Research*, 13(2), 159–168. [https://doi.org/10.1016/S0926-](https://doi.org/10.1016/S0926-6410(01)00104-5)
917 [6410\(01\)00104-5](https://doi.org/10.1016/S0926-6410(01)00104-5)
- 918 Heim, S., Amunts, K., Hensel, T., Grande, M., Huber, W., Binkofski, F., & Eickhoff, S. B.
919 (2012). The Role of Human Parietal Area 7A as a Link between Sequencing in Hand
920 Actions and in Overt Speech Production. *Frontiers in Psychology*, 3.
921 <https://doi.org/10.3389/fpsyg.2012.00534>

THE NEURAL CIRCUITRY UNDERLYING THE “RHYTHM EFFECT” IN STUTTERING

- 922 Hickok, G., Buchsbaum, B., Humphries, C., & Muftuler, T. (2003). Auditory–Motor Interaction
923 Revealed by fMRI: Speech, Music, and Working Memory in Area Spt. *Journal of*
924 *Cognitive Neuroscience*, 15(5), 673–682. <https://doi.org/10.1162/089892903322307393>
- 925 Hutchinson, J. M., & Norris, G. M. (1977). The differential effect of three auditory stimuli on the
926 frequency of stuttering behaviors. *Journal of Fluency Disorders*, 2(4), 283–293.
927 [https://doi.org/10.1016/0094-730X\(77\)90032-8](https://doi.org/10.1016/0094-730X(77)90032-8)
- 928 *IEEE Recommended Practice for Speech Quality Measurements* (No. 17; pp. 227–246). (1969).
929 IEEE Transactions on Audio and Electroacoustics.
930 <https://doi.org/10.1109/IEEESTD.1969.7405210>
- 931 Ingham, R. J., Fox, P. T., Costello Ingham, J., & Zamarripa, F. (2000). Is Overt Stuttered Speech
932 a Prerequisite for the Neural Activations Associated with Chronic Developmental
933 Stuttering? *Brain and Language*, 75(2), 163–194. <https://doi.org/10.1006/brln.2000.2351>
- 934 Ingham, R. J., Grafton, S. T., Bothe, A. K., & Ingham, J. C. (2012). Brain activity in adults who
935 stutter: Similarities across speaking tasks and correlations with stuttering frequency and
936 speaking rate. *Brain and Language*, 122(1), 11–24.
937 <https://doi.org/10.1016/j.bandl.2012.04.002>
- 938 Jackson, E. S., Yaruss, J. S., Quesal, R. W., Terranova, V., & Whalen, D. H. (2015). Responses
939 of adults who stutter to the anticipation of stuttering. *Journal of Fluency Disorders*, 45,
940 38–51. <https://doi.org/10.1016/j.jfludis.2015.05.002>
- 941 Jenkins, I., Brooks, D., Nixon, P., Frackowiak, R., & Passingham, R. (1994). Motor sequence
942 learning: A study with positron emission tomography. *The Journal of Neuroscience*,
943 14(6), 3775–3790. <https://doi.org/10.1523/JNEUROSCI.14-06-03775.1994>

THE NEURAL CIRCUITRY UNDERLYING THE “RHYTHM EFFECT” IN STUTTERING

- 944 Kell, C. A., Neumann, K., Behrens, M., von Gudenberg, A. W., & Giraud, A.-L. (2018).
945 Speaking-related changes in cortical functional connectivity associated with assisted and
946 spontaneous recovery from developmental stuttering. *Journal of Fluency Disorders*, *55*,
947 135–144. <https://doi.org/10.1016/j.jfludis.2017.02.001>
- 948 Kell, C. A., Neumann, K., von Kriegstein, K., Posenenske, C., von Gudenberg, A. W., Euler, H.,
949 & Giraud, A.-L. (2009). How the brain repairs stuttering. *Brain*, *132*(10), 2747–2760.
950 <https://doi.org/10.1093/brain/awp185>
- 951 Keuken, M. C., Bazin, P.-L., Crown, L., Hootsmans, J., Laufer, A., Müller-Axt, C., Sier, R., van
952 der Putten, E. J., Schäfer, A., Turner, R., & Forstmann, B. U. (2014). Quantifying inter-
953 individual anatomical variability in the subcortex using 7 T structural MRI. *NeuroImage*,
954 *94*, 40–46. <https://doi.org/10.1016/j.neuroimage.2014.03.032>
- 955 Krauth, A., Blanc, R., Poveda, A., Jeanmonod, D., Morel, A., & Székely, G. (2010). A mean
956 three-dimensional atlas of the human thalamus: Generation from multiple histological
957 data. *NeuroImage*, *49*(3), 2053–2062. <https://doi.org/10.1016/j.neuroimage.2009.10.042>
- 958 Lee, A., & Kawahara, T. (2009, January). Recent Development of Open-Source Speech
959 recognition Engine Julius. *Asia-Pacific Signal and Information Processing Association*,
960 *2009 Annual Summit and Conference*.
- 961 Lu, C., Chen, C., Ning, N., Ding, G., Guo, T., Peng, D., Yang, Y., Li, K., & Lin, C. (2010). The
962 neural substrates for atypical planning and execution of word production in stuttering.
963 *Experimental Neurology*, *221*(1), 146–156.
964 <https://doi.org/10.1016/j.expneurol.2009.10.016>
- 965 Lu, C., Chen, C., Peng, D., You, W., Zhang, X., Ding, G., Deng, X., Yan, Q., & Howell, P.
966 (2012). Neural anomaly and reorganization in speakers who stutter: A short-term

THE NEURAL CIRCUITRY UNDERLYING THE “RHYTHM EFFECT” IN STUTTERING

- 967 intervention study. *Neurology*, 79(7), 625–632.
968 <https://doi.org/10.1212/WNL.0b013e31826356d2>
- 969 Lu, C., Ning, N., Peng, D., Ding, G., Li, K., Yang, Y., & Lin, C. (2009). The role of large-scale
970 neural interactions for developmental stuttering. *Neuroscience*, 161(4), 1008–1026.
971 <https://doi.org/10.1016/j.neuroscience.2009.04.020>
- 972 Lu, C., Peng, D., Chen, C., Ning, N., Ding, G., Li, K., Yang, Y., & Lin, C. (2010). Altered
973 effective connectivity and anomalous anatomy in the basal ganglia-thalamocortical
974 circuit of stuttering speakers. *Cortex*, 46(1), 49–67.
975 <https://doi.org/10.1016/j.cortex.2009.02.017>
- 976 Max, L. (2004). Stuttering and internal models for sensorimotor control: A theoretical
977 perspective to generate testable hypotheses. In B. Maassen, R. Kent, P. Hermann, & P.
978 Van Lieshout (Eds.), *Speech Motor Control: In Normal and Disordered Speech* (pp. 357–
979 387). Oxford University Press.
- 980 Max, L., Guenther, F. H., Gracco, V. L., Ghosh, S. S., & Wallace, M. E. (2004). Unstable or
981 Insufficiently Activated Internal Models and Feedback-Biased Motor Control as Sources
982 of Dysfluency: A Theoretical Model of Stuttering. *Contemporary Issues in*
983 *Communication Science and Disorders*, 31(Spring), 105–122.
984 https://doi.org/10.1044/cicsd_31_S_105
- 985 McLaren, D. G., Ries, M. L., Xu, G., & Johnson, S. C. (2012). A generalized form of context-
986 dependent psychophysiological interactions (gPPI): A comparison to standard
987 approaches. *NeuroImage*, 61(4), 1277–1286.
988 <https://doi.org/10.1016/j.neuroimage.2012.03.068>

THE NEURAL CIRCUITRY UNDERLYING THE “RHYTHM EFFECT” IN STUTTERING

- 989 Morris, L. S., Kundu, P., Dowell, N., Mechelmans, D. J., Favre, P., Irvine, M. A., Robbins, T.
990 W., Daw, N., Bullmore, E. T., Harrison, N. A., & Voon, V. (2016). Fronto-striatal
991 organization: Defining functional and microstructural substrates of behavioural
992 flexibility. *Cortex*, *74*, 118–133. <https://doi.org/10.1016/j.cortex.2015.11.004>
- 993 Neumann, K., Euler, H. A., Gudenberg, A. W. von, Giraud, A.-L., Lanfermann, H., Gall, V., &
994 Preibisch, C. (2003). The nature and treatment of stuttering as revealed by fMRI. *Journal*
995 *of Fluency Disorders*, *28*(4), 381–410. <https://doi.org/10.1016/j.jfludis.2003.07.003>
- 996 Neumann, K., Preibisch, C., Euler, H. A., Gudenberg, A. W. von, Lanfermann, H., Gall, V., &
997 Giraud, A.-L. (2005). Cortical plasticity associated with stuttering therapy. *Journal of*
998 *Fluency Disorders*, *30*(1), 23–39. <https://doi.org/10.1016/j.jfludis.2004.12.002>
- 999 Nieto-Castañón, A. (2020). *Handbook of functional connectivity Magnetic resonance Imaging*
1000 *methods in CONN*. Hilbert Press.
- 1001 Ochsner, K. N., Silvers, J. A., & Buhle, J. T. (2012). Functional imaging studies of emotion
1002 regulation: A synthetic review and evolving model of the cognitive control of emotion:
1003 Functional imaging studies of emotion regulation. *Annals of the New York Academy of*
1004 *Sciences*, *1251*(1), E1–E24. <https://doi.org/10.1111/j.1749-6632.2012.06751.x>
- 1005 Oldfield, R. C. (1971). The assessment and analysis of handedness: The Edinburgh inventory.
1006 *Neuropsychologia*, *9*(1), 97–113.
- 1007 Parkinson, A. L., Flagmeier, S. G., Manes, J. L., Larson, C. R., Rogers, B., & Robin, D. A.
1008 (2012). Understanding the neural mechanisms involved in sensory control of voice
1009 production. *NeuroImage*, *61*(1), 314–322.
1010 <https://doi.org/10.1016/j.neuroimage.2012.02.068>

THE NEURAL CIRCUITRY UNDERLYING THE “RHYTHM EFFECT” IN STUTTERING

- 1011 Pellegrino, F., Coupé, C., & Marsico, E. (2011). Across-Language Perspective on Speech
1012 Information Rate. *Language*, *87*(3), 539–558. <https://doi.org/10.1353/lan.2011.0057>
- 1013 Pellegrino, F., Farinas, J., & Rouas, J.-L. (2004). Automatic Estimation of Speaking Rate in
1014 Multilingual Spontaneous Speech. *Speech Prosody 2004*, 517–520.
- 1015 Preibisch, C., Neumann, K., Raab, P., Euler, H. A., von Gudenberg, A. W., Lanfermann, H., &
1016 Giraud, A.-L. (2003). Evidence for compensation for stuttering by the right frontal
1017 operculum. *NeuroImage*, *20*(2), 1356–1364. <https://doi.org/10.1016/S1053->
1018 [8119\(03\)00376-8](https://doi.org/10.1016/S1053-8119(03)00376-8)
- 1019 Riecker, A., Kassubek, J., Gröschel, K., Grodd, W., & Ackermann, H. (2006). The cerebral
1020 control of speech tempo: Opposite relationship between speaking rate and BOLD signal
1021 changes at striatal and cerebellar structures. *NeuroImage*, *29*(1), 46–53.
1022 <https://doi.org/10.1016/j.neuroimage.2005.03.046>
- 1023 Riley, G. D. (2008). *SSI-4, Stuttering severity instrument for children and adults* (4th ed.). Pro Ed.
- 1024 Rottschy, C., Langner, R., Dogan, I., Reetz, K., Laird, A. R., Schulz, J. B., Fox, P. T., &
1025 Eickhoff, S. B. (2012). Modelling neural correlates of working memory: A coordinate-
1026 based meta-analysis. *NeuroImage*, *60*(1), 830–846.
1027 <https://doi.org/10.1016/j.neuroimage.2011.11.050>
- 1028 Salmelin, R., Schnitzler, A., Schmitz, F., & Freund, H.-J. (2000). Single word reading in
1029 developmental stutterers and fluent speakers. *Brain*, *123*(6), 1184–1202.
1030 <https://doi.org/10.1093/brain/123.6.1184>
- 1031 Schubotz, R. I., & von Cramon, D. Y. (2001). Interval and Ordinal Properties of Sequences Are
1032 Associated with Distinct Premotor Areas. *Cerebral Cortex*, *11*(3), 210–222.
1033 <https://doi.org/10.1093/cercor/11.3.210>

THE NEURAL CIRCUITRY UNDERLYING THE “RHYTHM EFFECT” IN STUTTERING

- 1034 Segawa, J. A., Tourville, J. A., Beal, D. S., & Guenther, F. H. (2015). The Neural Correlates of
1035 Speech Motor Sequence Learning. *Journal of Cognitive Neuroscience*, 27(4), 819–831.
1036 https://doi.org/10.1162/jocn_a_00737
- 1037 Shuster, L., & Lemieux, S. (2005). An fMRI investigation of covertly and overtly produced
1038 mono- and multisyllabic words. *Brain and Language*, 93(1), 20–31.
1039 <https://doi.org/10.1016/j.bandl.2004.07.007>
- 1040 Sitek, K. R., Cai, S., Beal, D. S., Perkell, J. S., Guenther, F. H., & Ghosh, S. S. (2016).
1041 Decreased Cerebellar-Orbitofrontal Connectivity Correlates with Stuttering Severity:
1042 Whole-Brain Functional and Structural Connectivity Associations with Persistent
1043 Developmental Stuttering. *Frontiers in Human Neuroscience*, 10.
1044 <https://doi.org/10.3389/fnhum.2016.00190>
- 1045 Stager, S. V., Denman, D. W., & Ludlow, C. L. (1997). Modifications in Aerodynamic Variables
1046 by Persons Who Stutter Under Fluency-Evoking Conditions. *Journal of Speech,*
1047 *Language, and Hearing Research*, 40(4), 832–847. <https://doi.org/10.1044/jslhr.4004.832>
- 1048 Stager, S. V., Jeffries, K. J., & Braun, A. R. (2003). Common features of fluency-evoking
1049 conditions studied in stuttering subjects and controls: An PET study. *Journal of Fluency*
1050 *Disorders*, 28(4), 319–336. <https://doi.org/10.1016/j.jfludis.2003.08.004>
- 1051 Strick, P. L., Dum, R. P., & Fiez, J. A. (2009). Cerebellum and Nonmotor Function. *Annual*
1052 *Review of Neuroscience*, 32(1), 413–434.
1053 <https://doi.org/10.1146/annurev.neuro.31.060407.125606>
- 1054 Takaso, H., Eisner, F., Wise, R. J. S., & Scott, S. K. (2010). The Effect of Delayed Auditory
1055 Feedback on Activity in the Temporal Lobe While Speaking: A Positron Emission

THE NEURAL CIRCUITRY UNDERLYING THE “RHYTHM EFFECT” IN STUTTERING

- 1056 Tomography Study. *Journal of Speech, Language, and Hearing Research*, 53(2), 226–
1057 236. [https://doi.org/10.1044/1092-4388\(2009/09-0009\)](https://doi.org/10.1044/1092-4388(2009/09-0009))
- 1058 Teki, S., Grube, M., & Griffiths, T. D. (2012). A Unified Model of Time Perception Accounts
1059 for Duration-Based and Beat-Based Timing Mechanisms. *Frontiers in Integrative*
1060 *Neuroscience*, 5. <https://doi.org/10.3389/fnint.2011.00090>
- 1061 Tourville, J. A., Reilly, K. J., & Guenther, F. H. (2008). Neural mechanisms underlying auditory
1062 feedback control of speech. *NeuroImage*, 39(3), 1429–1443.
1063 <https://doi.org/10.1016/j.neuroimage.2007.09.054>
- 1064 Toyomura, A., Fujii, T., & Kuriki, S. (2011). Effect of external auditory pacing on the neural
1065 activity of stuttering speakers. *NeuroImage*, 57(4), 1507–1516.
1066 <https://doi.org/10.1016/j.neuroimage.2011.05.039>
- 1067 Toyomura, A., Fujii, T., & Kuriki, S. (2015). Effect of an 8-week practice of externally triggered
1068 speech on basal ganglia activity of stuttering and fluent speakers. *NeuroImage*, 109, 458–
1069 468. <https://doi.org/10.1016/j.neuroimage.2015.01.024>
- 1070 Van Borsel, J., Achten, E., Santens, P., Lahorte, P., & Voet, T. (2003). fMRI of developmental
1071 stuttering: A pilot study. *Brain and Language*, 85(3), 369–376.
1072 [https://doi.org/10.1016/S0093-934X\(02\)00588-6](https://doi.org/10.1016/S0093-934X(02)00588-6)
- 1073 Wager, T. D., & Smith, E. E. (2003). Neuroimaging studies of working memory: *Cognitive,*
1074 *Affective, & Behavioral Neuroscience*, 3(4), 255–274.
1075 <https://doi.org/10.3758/CABN.3.4.255>
- 1076 Watkins, K. E., Smith, S. M., Davis, S., & Howell, P. (2007). Structural and functional
1077 abnormalities of the motor system in developmental stuttering. *Brain*, 131(1), 50–59.
1078 <https://doi.org/10.1093/brain/awm241>

THE NEURAL CIRCUITRY UNDERLYING THE “RHYTHM EFFECT” IN STUTTERING

- 1079 Whitfield-Gabrieli, S., & Nieto-Castanon, A. (2012). Conn: A Functional Connectivity Toolbox
1080 for Correlated and Anticorrelated Brain Networks. *Brain Connectivity*, 2(3), 125–141.
1081 <https://doi.org/10.1089/brain.2012.0073>
- 1082 Wiener, M., Turkeltaub, P., & Coslett, H. B. (2010). The image of time: A voxel-wise meta-
1083 analysis. *NeuroImage*, 49(2), 1728–1740.
1084 <https://doi.org/10.1016/j.neuroimage.2009.09.064>
- 1085 Yairi, E., & Ambrose, N. G. (1999). Early Childhood Stuttering I: Persistency and Recovery
1086 Rates. *Journal of Speech Language and Hearing Research*, 42(5), 1097.
1087 <https://doi.org/10.1044/jslhr.4205.1097>
- 1088 Zeid, O., & Bullock, D. (2019). Moving in time: Simulating how neural circuits enable rhythmic
1089 enactment of planned sequences. *Neural Networks*, 120, 86–107.
1090 <https://doi.org/10.1016/j.neunet.2019.08.006>
1091

THE NEURAL CIRCUITRY UNDERLYING THE “RHYTHM EFFECT” IN STUTTERING

1092
1093
1094
1095
1096
1097
1098
1099
1100
1101
1102
1103
1104
1105
1106
1107
1108
1109
1110

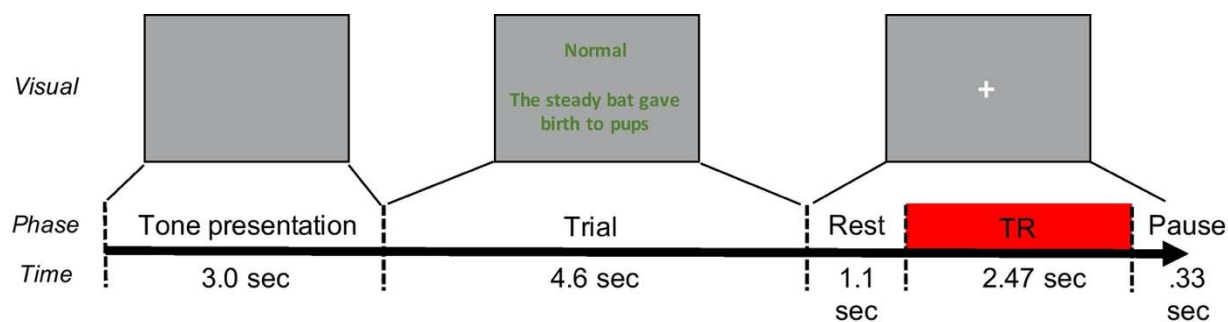
Appendix

Stimulus sentences used in the present experiment

1. Rice is often served in round bowls.
2. The juice of lemons makes fine punch.
3. The boy was there when the sun rose.
4. Her purse was full of useless trash.
5. Hoist the load to your left shoulder.
6. The young girl gave no clear response.
7. Sickness kept him home the third week.
8. Lift the square stone over the fence.
9. The friendly gang left the drug store.
10. The lease ran out in sixteen weeks.
11. The steady bat gave birth to pups.
12. There are more than two factors here.
13. The lawyer tried to lose his case.
14. The term ended late June that year.
15. The pipe began to rust while new.
16. Act on these orders with great speed.

THE NEURAL CIRCUITRY UNDERLYING THE “RHYTHM EFFECT” IN STUTTERING

1111 **Figure 1:** Schematic diagram illustrating the temporal structure of stimulus presentation during
1112 functional data acquisition. At the start of each trial, isochronous tone sequences were presented
1113 for 3.0 seconds. The visual stimulus then appeared and remained on screen for 4.6 seconds. 1.1
1114 seconds after stimulus offset, a whole-brain volume was acquired. The next trial started 0.33
1115 seconds after data acquisition was complete. TR = repetition time.

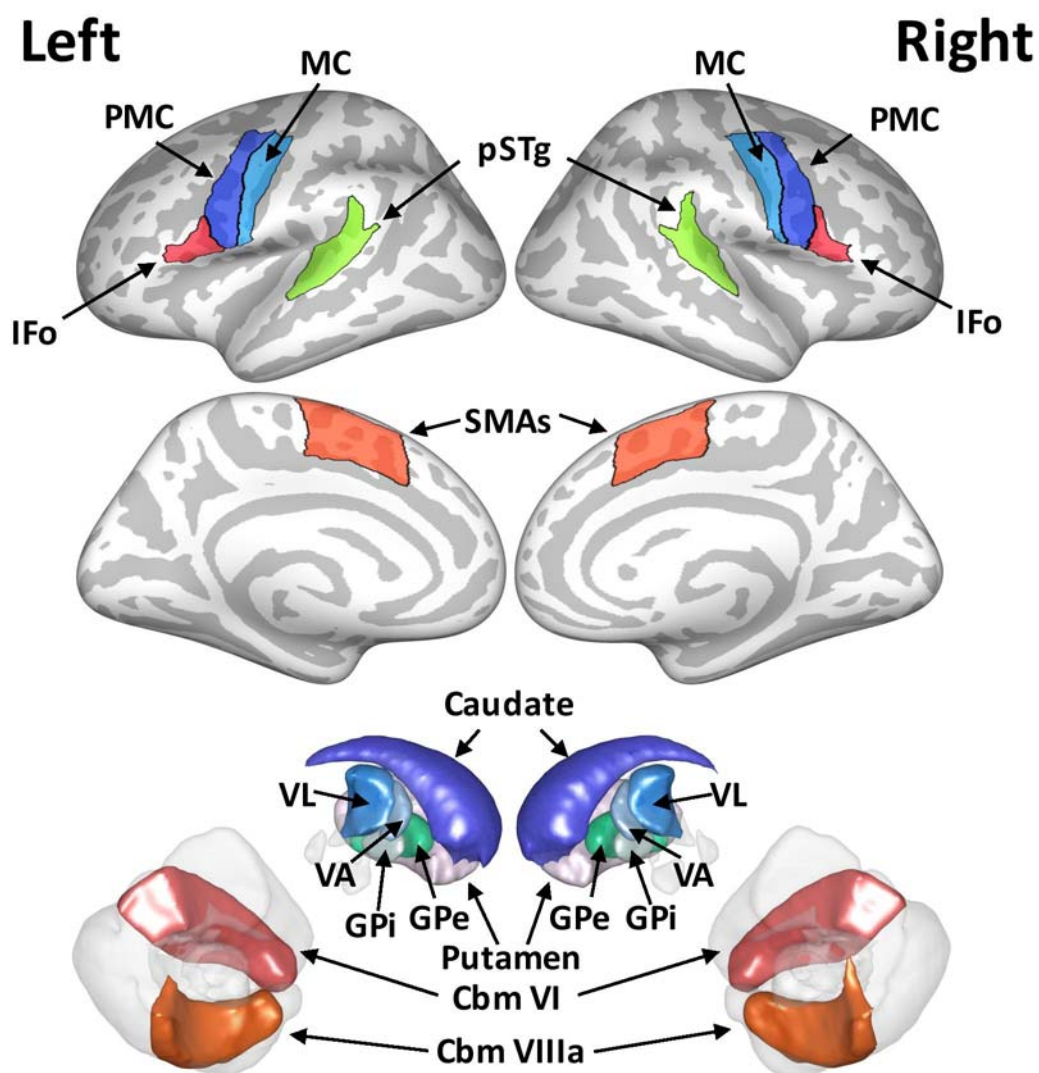


1116

1117

THE NEURAL CIRCUITRY UNDERLYING THE “RHYTHM EFFECT” IN STUTTERING

1118 **Figure 2:** Regions of interest included in the primary hypothesis-based analysis. Cortical regions
1119 are displayed on an inflated cortical surface, while subcortical and cerebellar regions are
1120 rendered in 3-D volume space. IFo = grouped dorsal and ventral inferior frontal gyrus pars
1121 operularis, PMC = grouped ventral and mid premotor cortex, MC = grouped ventral and mid
1122 motor cortex, pSTg = grouped posterior superior temporal gyrus, SMAs = grouped
1123 supplementary motor areas, VL = ventrolateral thalamic nucleus, VA = ventroanterior thalamic
1124 nucleus, GPi = internal portion of globus pallidus, GPe = external portion of globus pallidus,
1125 Cbm VI = cerebellum lobule VI, Cbm VIIIa = cerebellum lobule VIIIa.



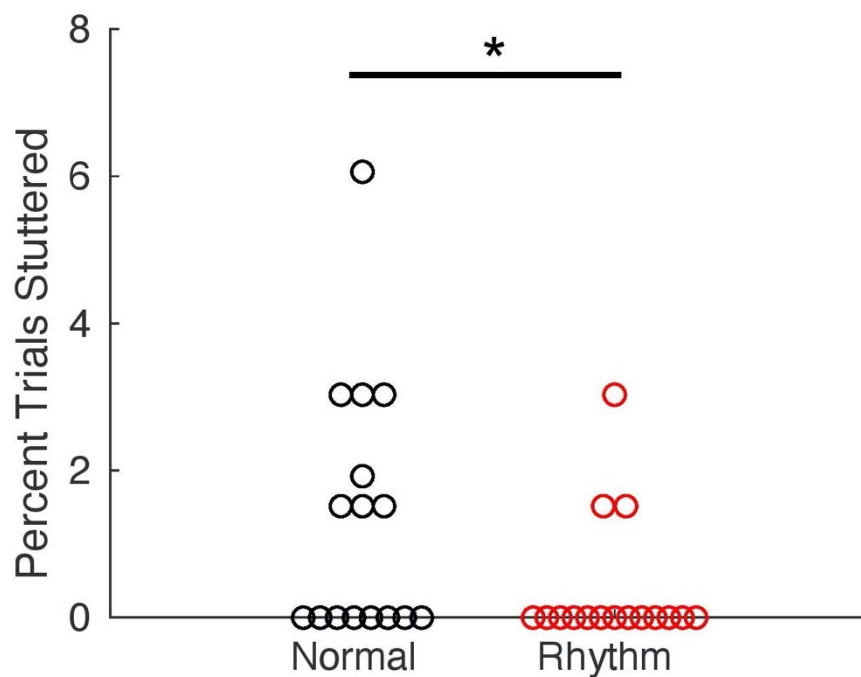
1126

THE NEURAL CIRCUITRY UNDERLYING THE “RHYTHM EFFECT” IN STUTTERING

1127 **Figure 3:** Comparison of dysfluencies between the normal and rhythm conditions for AWS.

1128 Circles represent individual participants. * $p < 0.05$.

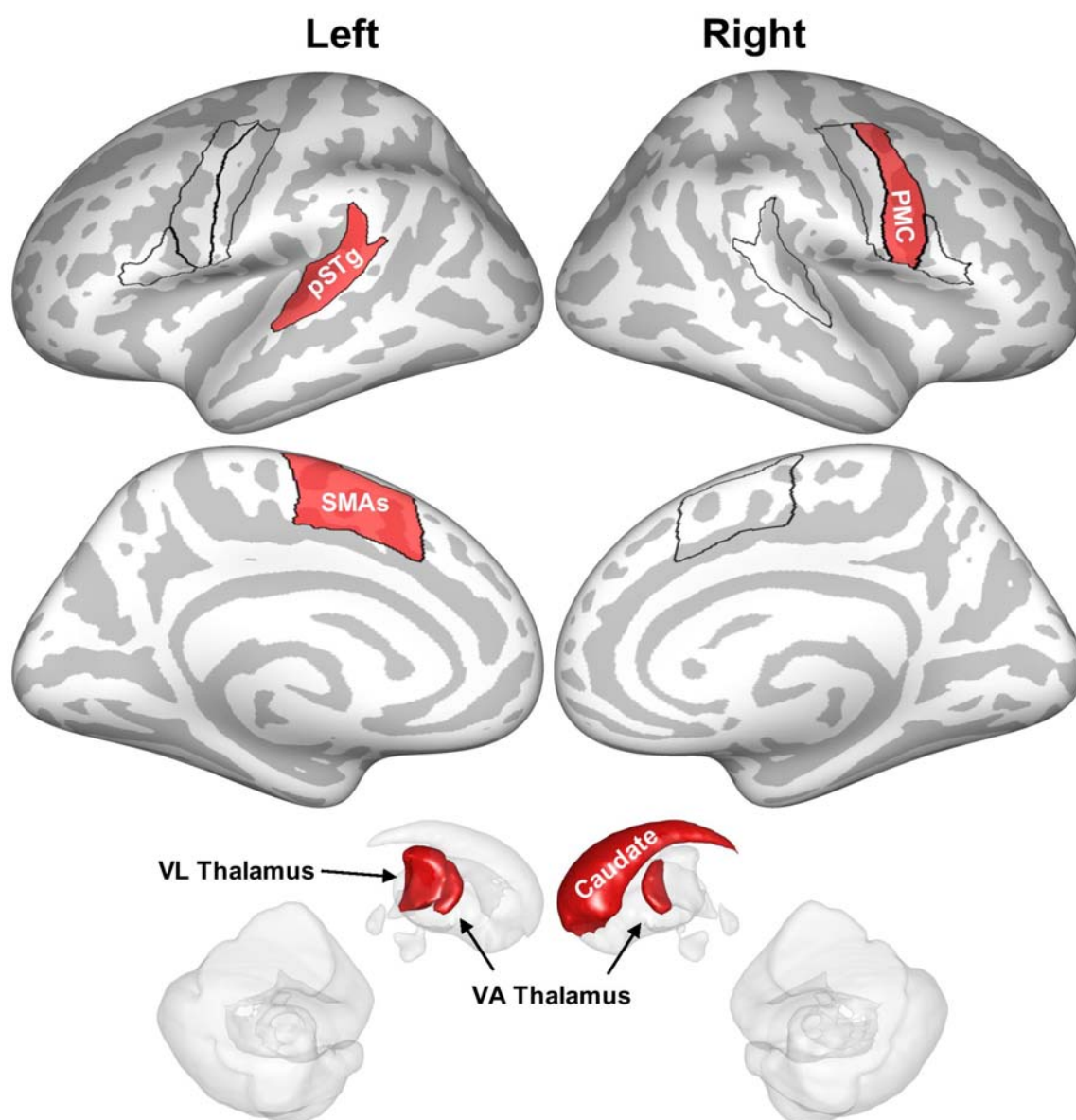
1129



1130

THE NEURAL CIRCUITRY UNDERLYING THE “RHYTHM EFFECT” IN STUTTERING

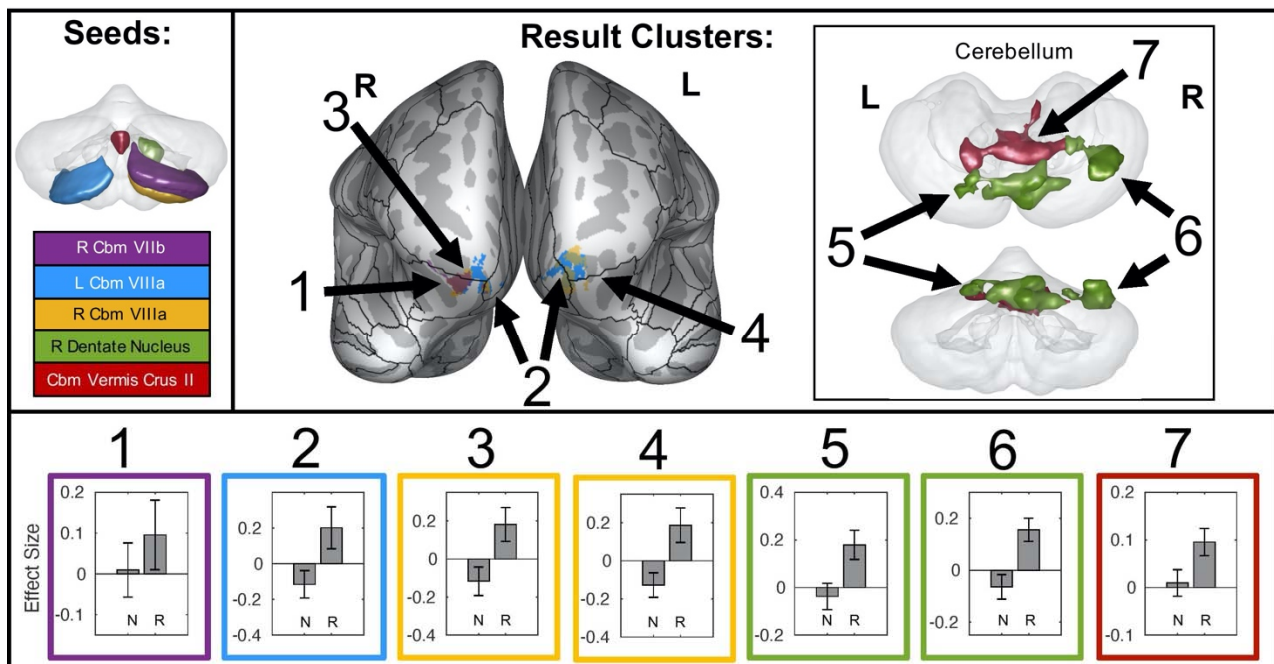
1131 **Figure 4:** Primary regions-of-interest (ROIs) significantly more active during the rhythmic
1132 condition than the normal condition for ANS in the primary analysis ($pFDR < 0.05$) are
1133 highlighted in red and plotted on an inflated cortical surface or on a 3-D rendering of subcortical
1134 structures. Black outlines indicate cortical ROIs included in the primary analysis (as in Figure 2).
1135 pSTg = posterior superior temporal gyrus, SMAs = grouped supplementary motor areas, PMC =
1136 grouped ventral and mid premotor cortex, pSTg = grouped posterior superior temporal gyrus and
1137 planum temporale, VA = ventro-anterior, VL = ventro-lateral.



1138

THE NEURAL CIRCUITRY UNDERLYING THE “RHYTHM EFFECT” IN STUTTERING

1139 **Figure 5:** A summary of functional connections that are significantly different between the
1140 normal and rhythm conditions in AWS. Seed regions for these connections are indicated in the
1141 upper left corner on a transparent 3D rendering of the cerebellum (viewed posteriorly), and
1142 colors in the rest of the figure refer back to these seed regions. Seven target clusters (representing
1143 7 distinct connections) are displayed in the upper right portion of the figure. Target clusters 1-4
1144 are projected onto an inflated surface of cerebral cortex, along with the full cortical ROI
1145 parcellation of the SpeechLabel atlas described in Cai et al. (2014). Target clusters 5, 6 and 7 are
1146 displayed on a transparent 3D rendering of the cerebellum (top view: superior; bottom view:
1147 posterior). The bottom portion of the figure shows the connectivity effect sizes in the normal and
1148 rhythm conditions for each connection. Error bars indicate 90% confidence intervals. N =
1149 normal, R = rhythm, L = left, R = right, Cbm = cerebellum.

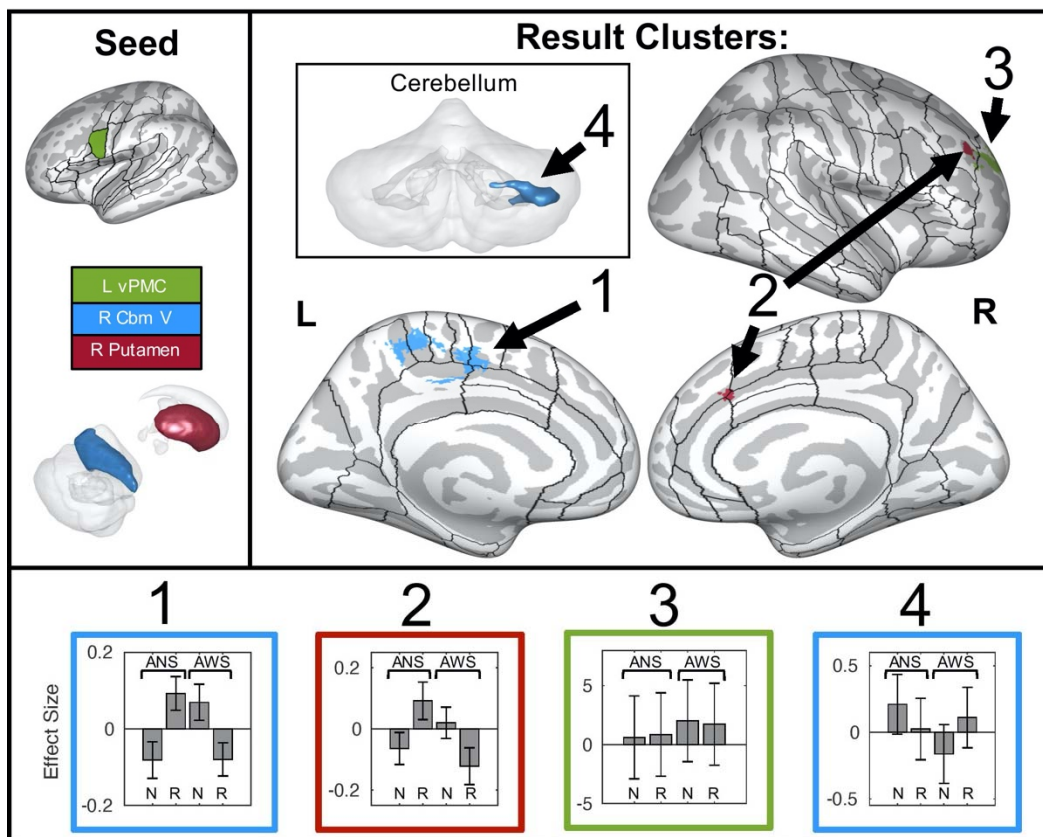


1150

1151

THE NEURAL CIRCUITRY UNDERLYING THE “RHYTHM EFFECT” IN STUTTERING

1152 **Figure 6:** A summary of functional connections that show significant interactions between group
1153 and condition. Seed regions for these connections are indicated in the upper left panel on an
1154 inflated cortical surface (top; ROIs are as in Figure 2) or on a transparent 3D rendering of the
1155 cerebellum and subcortical structures viewed from the right (bottom). Colors in the rest of the
1156 figure refer back to these seed regions. Four target clusters (representing 4 distinct connections)
1157 are displayed in the upper right portion of the figure. Target clusters 1, 2, and 3 are projected
1158 onto an inflated surface of cerebral cortex, along with the full cortical ROI parcellation of the
1159 SpeechLabel atlas described in Cai et al. (2014). Target cluster 4 is displayed on a transparent 3D
1160 rendering of the cerebellum (posterior view). The bottom portion of the figure shows the
1161 connectivity effect sizes for each connection in the normal and rhythm conditions, separately for
1162 each group. Error bars indicate 90% confidence intervals. N = normal, R = rhythm, L = left, R =
1163 right, vPMC = ventral premotor cortex, Cbm = cerebellum.



1164

THE NEURAL CIRCUITRY UNDERLYING THE “RHYTHM EFFECT” IN STUTTERING

1165 **Table 1:** Demographic and stuttering severity data from adults who stutter. F = female; M =
1166 male; SSI-4 = Stuttering Severity Index – Fourth Edition. SSI-Mod = a modified version of the
1167 SSI-4 that does not include a subscore related to concomitant movements. Disfluency Rate = the
1168 percent of trials containing disfluencies during the Normal speech condition.

Subject ID	Age	Gender	SSI-4 Composite	SSI-Mod	Disfluency Rate
AWS01	19	F	28	19	0%
AWS02	22	F	31	26	3.03%
AWS03	31	F	30	22	3.03%
AWS04	21	M	9	7	1.92%
AWS05	58	M	14	11	0%
AWS06	23	M	42	29	0%
AWS07	53	M	27	22	0%
AWS08	44	M	20	16	0%
AWS09	20	M	18	15	1.52%
AWS10	22	M	27	18	3.02%
AWS11	21	M	19	16	6.06%
AWS12	20	M	24	14	1.52%
AWS13	29	M	33	28	*Missing Data
AWS14	18	F	14	11	0%
AWS15	35	M	30	19	0%
AWS16	42	M	22	17	1.52%
AWS17	29	M	14	12	0%

1169

1170

THE NEURAL CIRCUITRY UNDERLYING THE “RHYTHM EFFECT” IN STUTTERING

1171 **Table 2:** Primary regions-of-interest with activation differences between the rhythm and normal
1172 conditions for ANS and AWS ($p < 0.05$). * indicates regions that survive a significance threshold
1173 of $pFDR < 0.05$ for their respective analyses, unc = uncorrected, SMA = grouped supplementary
1174 motor areas, PMC = grouped ventral and mid premotor cortex, pSTg = grouped posterior
1175 superior temporal gyrus and planum temporale, VA = ventroanterior thalamic nucleus, VL =
1176 ventral lateral thalamic nucleus.

ROI	Hemisphere	<i>t-value</i>	<i>p-unc</i>
<i>ANS, Rhythm > Normal</i>			
SMA _s	Left	4.68	0.0004*
PMC	Right	3.22	0.0062*
pSTg	Left	2.94	0.0108*
VA	Left	3.88	0.0017*
	Right	2.98	0.0098*
VL	Left	3.59	0.0030*
Caudate	Right	3.72	0.0023*

1177

1178

THE NEURAL CIRCUITRY UNDERLYING THE “RHYTHM EFFECT” IN STUTTERING

1179 **Table 3:** Primary regions-of-interest with significant correlations between severity measures and
1180 speech activation in AWS ($p < 0.05$). * indicates regions that survive a significance threshold of
1181 $pFDR < 0.05$ for their respective analyses, unc = uncorrected, VA = ventroanterior thalamic
1182 nucleus, VL = ventrolateral thalamic nucleus.

ROI	Hemisphere	<i>t-value</i>	<i>p-unc</i>
<i>Normal-Baseline Correlation with Disfluency Rate</i>			
VA	Left	4.15	0.0013*
VL	Left	3.43	0.0049*
	Right	3.44	0.0049*

1183

1184

1185 **Table 4:** Functional connectivity analysis results. ROI = region-of-interest, MNI = Montreal Neurological Institute, FDR = false
1186 discovery rate, L = left, R = right, Cbm = cerebellum, FP = frontal pole, FMC = fronto-medial cortex; FOC = fronto-orbital cortex,
1187 SCC = subcallosal cortex, Inter = interposed nucleus, Den = dentate nucleus, vCMA = ventral cingulate motor area, dCMA = dorsal
1188 cingulate motor area, ACC = anterior cingulate cortex, OC = occipital cortex, LG = lingual gyrus, TOFG = temporo-occipital fusiform
1189 gyrus, SPL = superior parietal lobule, PCN = precuneus AG = angular gyrus, aMFG = anterior middle frontal gyrus, SFG = superior
1190 frontal gyrus, preSMA = presupplementary motor area, MC = primary motor cortex, SC = somatosensory cortex, SMA =
1191 supplementary motor area, PCC = posterior cingulate cortex, SPL = superior parietal lobule.

THE NEURAL CIRCUITRY UNDERLYING THE “RHYTHM EFFECT” IN STUTTERING

Seed ROI	Target Cluster Regions	Peak MNI Coordinates (x,y,z)			Cluster Size (# of Voxels)	p-FDR
<i>AWS, Rhythm > Normal</i>						
L Cbm VIIIa	Midline Orbitofrontal Cortex (L FP, L FMC, R FP, R FOC, R FMC, L FOC, L SCC)	-4	44	-24	785	< 1 x 10 ⁻⁶
R Cbm VIIIa	Left Orbitofrontal Cortex (L FP, L FMC, L FOC)	-6	38	-24	361	< 1 x 10 ⁻⁶
	Right Orbitofrontal Cortex (R FOC, R FP, R FMC)	30	38	-20	381	< 1 x 10 ⁻⁶
R Cbm VIIb	Right Orbitofrontal Cortex (R FOC, R FP, R FMC)	16	42	-24	269	0.000006
R Dentate Nucleus	Superior cerebellum (Ver VI, R VI, L VI, R Crus I, L Crus I, R Crus II)	8	-82	-22	402	< 1 x 10 ⁻⁶
	Right Superior Cerebellum (R VI, R Crus I)	36	-60	-24	215	0.000052
Cbm Vermis Crus II	Superior cerebellum (L VI, R VI, R V, L V, R I-IV, Ver VI, L I-IV, R Inter, L Inter, R Den)	8	-60	-22	354	< 1 x 10 ⁻⁶
<i>ANS, Rhythm > Normal</i>						
L VA Thalamus	Right Occipital Cortex (R LG, R TOFG, R Cbm VI, R OC, Ver VI)	32	-70	-10	163	0.000442
R preSMA	Left Parieto-Occipital Cortex (L SPL, L OC, L PCN, L AG)	-16	-70	32	212	0.000150
<i>ANS, Normal > Rhythm</i>						
L Substantia Nigra	Left Occipital Cortex (L OC)	-16	-92	-8	189	0.000216
<i>Group x Condition Interaction</i>						
L vPMC	Right Prefrontal Cortex (R FP, R aMFG, R SFg)	20	54	24	290	0.000035
R Putamen	Right Prefrontal Cortex (R aMFG, R dCMA, R SFg, R FP, R ACC)	22	22	30	212	0.000426
R Cbm V	Right Posterior Cerebellum (R Cbm Crus I, R Cbm Crus II, R Cbm VIIIa, R Cbm Den)	44	-58	-42	400	0.000005
	Left Medial Sensorimotor Cortex (L medial SC, L SMA, L PCN, L medial PMC, L medial MC, L PCC, L dCMA, R medial PMC, L SPL)	2	-14	48	351	0.000010

1192

bioRxiv preprint doi: <https://doi.org/10.1101/2020.10.27.350975>; this version posted October 28, 2020. The copyright holder for this preprint (which was not certified by peer review) is the author/funder. All rights reserved. No reuse allowed without permission.